Available online at www.sciencedirect.com
SCIENCE DIRECT®
Lithos 79 (2005) 317–341
LITHOS
www.elsevier.com/locate/lithos

Biotic effects of late Maastrichtian mantle plume volcanism: implications for impacts and mass extinctions

Gerta Keller*

Department of Geosciences, Princeton University, Princeton, NJ 08544, United States

Received 31 August 2003; accepted 9 September 2004
Available online 2 November 2004

Abstract

During the late Maastrichtian, DSDP Site 216 on Ninetyeast Ridge, Indian Ocean, passed over a mantle plume leading to volcanic eruptions, islands built to sea level, and catastrophic environmental conditions for planktic and benthic foraminifera. The biotic effects were severe, including dwarfing of all benthic and planktic species, a 90% reduction in species diversity, exclusion of all ecological specialists, near-absence of ecological generalists, and dominance of the disaster opportunist *Guembelitria* alternating with low O_2-tolerant species. These faunal characteristics are identical to those of the K–T boundary mass extinction, except that the fauna recovered after Site 216 passed beyond the influence of mantle plume volcanism about 500 kyr before the K–T boundary. Similar biotic effects have been observed in Madagascar, Israel, and Egypt. The direct correlation between mantle plume volcanism and biotic effects on Ninetyeast Ridge and the similarity to the K–T mass extinction, which is generally attributed to a large impact, reveal that impacts and volcanism can cause similar environmental catastrophes. This raises the inevitable question: Are mass extinctions caused by impacts or mantle plume volcanism? The unequivocal correlation between intense volcanism and high-stress assemblages necessitates a review of current impact and mass extinction theories.

Keywords: Volcanism; Impacts; Biotic effects; Late Maastrichtian; DSDP Site 216; Planktic foraminifera *Guembelitria*

1. Introduction

DSDP Site 216 was drilled on the crest of Ninetyeast Ridge just north of the equator at latitude 127.73′ N, longitude 90°12.48′ E, and at a water depth of 2237 m. During the late Maastrichtian, Site 216 was located at a paleolatitude of about 40°S on the crest of Ninetyeast Ridge, which consisted of islands built to sea level as the oceanic plate moved over a mantle plume, resulting in lithospheric uplift and volcanic deposition (Thompson et al., 1974; Moore et al., 1974). After passage over the mantle plume, the site rapidly subsided and deepened from shallow to deeper marine below the photic zone as Site 216 passed beyond the influence of mantle plume volcanism and chalk deposition resumed during the last 500 kyr of the Maastrichtian.

* Tel.: +1 609 258 4117; fax: +1 609 258 1671.
E-mail address: gkeller@princeton.edu.

0024-4937/$ - see front matter © 2004 Elsevier B.V. All rights reserved.
doi:10.1016/j.lithos.2004.09.005

Microfossils associated with these volcanic-rich sediments reveal unusually low diversity and small size, which was originally attributed to a high-latitude location and dissolution effects (Gartner, 1974; Gartner et al., 1974; McGowran, 1974). However, planktic and benthic foraminiferal assemblages consist of rather fragile small specimens, which would be most affected by dissolution, and none of the larger more robust and dissolution-resistant species is present. This argues against dissolution as a deciding factor in the composition of these species assemblages. The paleolocation of Site 216 at about 40°S also argues against low species diversity due to high latitudes. In the Atlantic and Pacific oceans, faunal assemblages at similar latitudes reveal relatively high diversity and normal morphologies (Li and Keller, 1998a; Abramovich et al., 2002).

This suggests that major volcanism (e.g., large igneous provinces) and associated environmental changes are the likely cause for the high-stress impoverished faunal assemblages at Site 216. Flood basalts are generally linked to hot spots, or superheated mantle plumes, which are believed to erupt over periods of 1–3 million years. During the late Maastrichtian in the Indian Ocean, both Reunion and Ninetyeast Ridge were active hot spots (Fig. 1).

Biotic effects directly attributable to flood basalts are still poorly understood and difficult to evaluate. DSDP Site 216 provides an ideal locality to evaluate the biotic and environmental effects of mantle plume activity from inception to cessation and the restoration of normal marine environments. The fact that this mantle plume activity began about 2 myr before and ended about 500 kyr prior to the K–T boundary, and involved the same biotic assemblages as at K–T time, permits comparison with the K–T mass extinction. High-stress planktic foraminiferal assemblages were recently also discovered in upper Maastrichtian sediments of Madagascar (Abramovich et al., 2002), Israel (Keller, 2004), Central Egypt (Keller, 2002), and Tunisia (Abramovich and Keller, 2002). These pre-K–T biotic catastrophes of yet unknown source and paleogeographic extent could also be linked to Deccan Traps or Ninetyeast Ridge volcanism in the Indian Ocean.

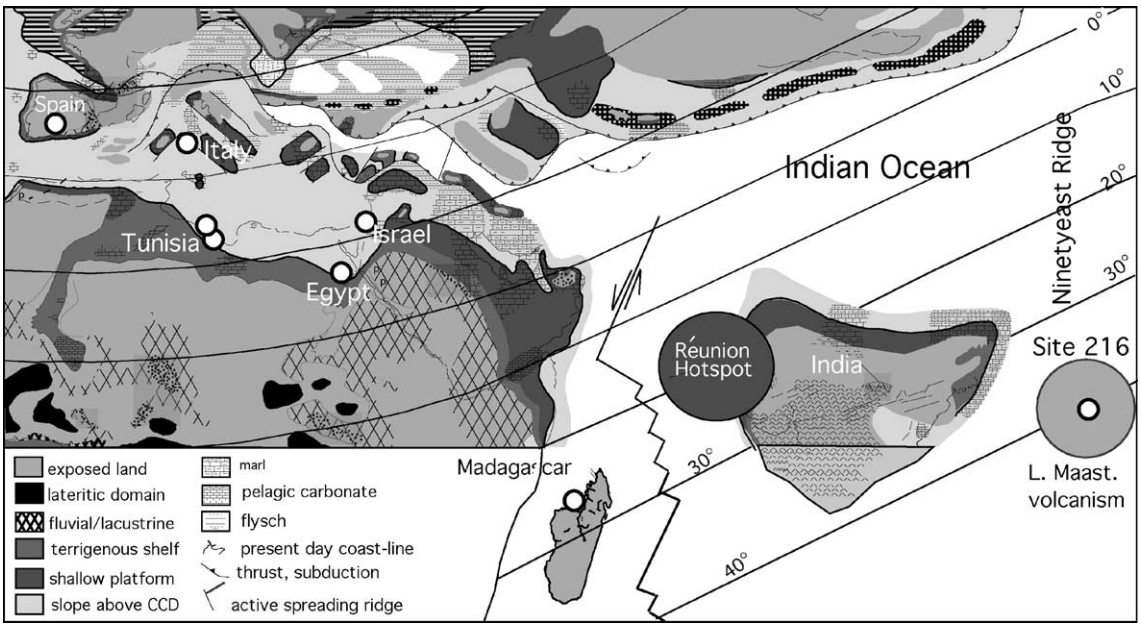

Fig. 1. Paleoenvironmental map of the Indian Ocean and eastern Tethys modified after Dercourt et al. (1993) with areas of plume activity shaded (reunion hotspot and Ninetyeast Ridge). Paleolocations of DSDP Site 216 and localities with similar high-stress planktic foraminiferal assemblages in Madagascar, Israel, Egypt, and Tunisia are indicated. Note that biotic effects of mantle plume volcanism decrease westward from the Indian Ocean to the eastern Tethys, with little expression in Tunisia and none in Spain.

This study quantifies and evaluates the biotic effects of late Maastrichtian mantle plume activity at DSDP Site 216 based on planktic and benthic foraminifera and compares these with the biotic effects observed in previous studies of Madagascar, Israel, Egypt, and Tunisia. Planktic foraminifera are unicellular species living in the upper water column and are highly sensitive to environmental changes. They suffered the most severe losses during the K–T boundary mass extinction and are therefore ideal markers for evaluating biotic effects of catastrophic events, whether volcanism or impacts.

2. Methods

A total of 88 samples were analyzed from Site 216 spanning from the basement basalt to the early Tertiary (cores 36–23). Fifty-eight samples yielded sufficient planktic foraminifera for quantitative analysis. Samples were processed following the standard method of Keller et al. (1995) and washed through a 63-μm screen, with the smaller (36–63 μm) size fraction separated and oven-dried for examination of tiny species. Planktic and benthic foraminifera at Site 216 are generally very small (<100 μm) and sparse below the chalk, although relatively well preserved, and test shells are little recrystallized. Dissolution effects are apparent in fragile tests.

Statistical counts of planktic foraminiferal species are based on random sample splits (using an Otto microsplitter) of about 150–250 specimens (average of 10 species) in the >63-μm size fraction. The smaller size fraction (36–63 μm) contains only rare specimens, and none is present in the >150-μm size fraction, except for the limestone interval at the top of the section. All specimens of the random aliquot were counted, picked, and mounted as permanent record on microslides and archived. The remaining sample residue was searched for rare species and these were recorded as part of the diversity, but not in the statistical counts. Because planktic foraminifera are relatively rare in these volcanic sediments, statistical counts in many samples are based on the entire residue of each sample with every specimen picked, counted, and identified (Table 1). Bias introduced by preservational effects (dissolution, breakage) appears to be minimal since the most fragile species (*Guembelitria*) are abundantly present and well preserved.

In each random sample split, benthic foraminifera were counted and recorded as ratio to planktic foraminifera and the taxa were identified. The remaining sample was searched for rare benthic species. Insufficient benthic foraminifera were recovered for quantitative analysis. Species identification follows standard taxonomic concepts (Robaszynski et al., 1984; Caron, 1985; Nederbragt, 1991, 1998; Von Morkhoven et al., 1986; Olsson et al., 1999).

3. Lithology and mineralogy

The basement rocks at Site 216 on Ninetyeast Ridge consist of a 20-m-thick unit of alternating vesicular basalt, amygdalar basalt, and homogenous basalt flows without pillow structures (Hekinian, 1974). The vesicularity of these basalts is attributed to a low-pressure extrusive environment, either subaerial or in shallow waters (Hekinian, 1974; Pimm, 1974), as also indicated by the presence of macrofaunas and microfaunas in the overlying units (Gartner et al., 1974; this study) (Fig. 2). Based on trace element analyses, the Ninetyeast Ridge basalts (Sites 216 and 214) are determined to be lower in Ca, Mg, Cr, and Ni concentrations, and higher in Fe, Ti, K, Ba, Cu, Sr, V, and Zr than midocean ridge basalts, island arc basalts, or basalts extruded on the ocean floor of the Indian Ocean, but very similar to Icelandic tholeitic basalts (Thompson et al., 1974, pp. 464–465). These authors therefore concluded that the Ninetyeast Ridge probably does not represent an old midocean ridge or island arc, but rather represents the surface expression of a former mantle plume with consequent uplift of the lithosphere as it moved over the hot spot.

The oldest sediments above the basalt consist of a 2.5-m-thick gray bioturbated clay-rich limestone mixed with altered (chloritized) volcanic debris (cores 36-2 and 36-3; Fig. 2). Above this unit is a 1.2-m-thick clayey micrite, also with chloritized volcanic debris (core 36-1). No glass is preserved in these sediments. Both units are bioturbated and contain abundant oysters and bivalve shell fragments, echinoid spines, shallow and deep water benthic foraminifera, and predominantly reworked planktic species.

Table 1
Relative percent abundances (>63 μm) of planktic foraminifera at DSDP Site 216, Ninetyeast Ridge, Indian Ocean

Biozone	CF1-2										CF3																			
Core section	23-3	24-2	24-2	24-3	24-3	24-4	24-4	24-5	24-5	25-1	25-2	25-3	25-4	26-1	26-2	26-3	27-1	27-2	28-1	28-1	28-1	28-2	28-3	28-3	28-3	29-1	29-2	29-2	29-2	
Interval (cm)	140	20	90	50	101	20	140	100	136	50	140	140	138	58	96	99	51	50	50	99	130	120	51	102	141	120	20	50	64	
Globigerinelloides aspera	18	19.6	19.7	28.2	6.8	7.6	18	25	14	17	5.7	7.8	2	5.2	3.1	3.1	x	6.3	1.5	2	3.3	3	5.6	1.7	x	3	3.8	1	5.5	
G. yaucoensis	3																													
Globotruncanella havanensis																														
G. petaloidea		1	1.6		1.8	1	1	x	x	1																				
G. subcarinatus			2.7	2.4	1.2	1.6	1	x																						
Hedbergella holmdelensis	6	4.5	3.8		8.1	2.7	5.6		2	1						1														
H. monmouthensis	5.2	7.8	6.5	3.2	5	5.5	4.7	x	6.9	2.7	3.3	3.6	1.5	1.4	11	6.3	11	16	6	11	4	2	13	8.8	4.8	7.7	3.8	4	1.3	
Rugoglobigerina rugosa	1.5	7.2	2.1	4.8	22	12	7.7	8.6	7.3	5.4	10	5.4	3.7	5.7	18	13	5.1	23	3.1	4	13	8	25	8.8	9.7	20	10	4.5	6	
Heterohelix globulosa	9	3.2	3.3	13.7	11.2	2.7	10	17	10	4.5	26	24.2	15	15	19	14,5	15	10	8.6	16	13	11	11	17	9.7	16	26	8.8	15	
H. dentata	18.6	17	19.7	15.3	19.7	20	14	20	16	16	18	22	22	26	11	22	28	8.6	17	16	12	20	20	13	6	25	9	23	6	
H. planata	3		3.8			9.8	6.7	1	10	1.8	5.7	7.3	2.6	4.2	6.2	3.9	2.3	x	x	2	10	1.8	6.6	3.5	3	6	10	1	x	
H. navarroensis	7.5	5.8	8.8	x	1.8	1	2	2.6	2.3	11	12	2	8.5	x	x	3.2	5.7	3.9	2.3	4	5.8	4.8	3.7	6.2	x	11	6.4	4	5.5	
P. cf costulata	12	19	14.8	x	1.8	9.3	4.7	3	x	9	x	2.4	5.8	x	4.2	5.7	1.2	5.3	5.5	1	6.6	2	2.8	5.3	x	4.7	3.8	1	1	
Guembelitria cretacea														x	x	x	11	5.5	45	32	17	38	4.7	21	57	1.5	21	49	47	
Guembelitria dammula							x											3.1	9.4	3.3	6.6	6			2.4				6.8	
Zeauvigerina waiparaensis	3.7	3.9	2.1	10.4	6.2	3.2	12	9.1	26	23	19	25	38	41	26	27	20	10	1.5	6.7	7.4	4	7.4	14	6	4.7	9	3	4	
Gublerina robusta	3.7	3.9	6.5	12.9	12	8.7	5.6	10	3	4.5				x	x	x														
P. deformis (=P. elegans)	2.2	x						x	x	x			x																	
P. hariaensis	4.5	4.5	2.7	1.6	x	3.2		x	x	x																				
P. palpebra	1.5	1.5	1	2,4	x	3.8	1	x	2.3	x																				
P. carseyae	x	x						x																						
A. cretacea					x			x																						
Globotruncana aegyptiaca								x																						
G. arca	x	1	x	4	x	4.8	x	1	x	1				x	x	x														
G. rosetta			x		x	1	x	x	x																					
G. insignis			x					x	x	x																				
G. contusa								x																						
G. stuarti						x	x																							
G. pettersi		x					x																							
G. conica						x		x																						
Abathomphalus mayaroensis		x	x		x	x	x	1	x	x																				
Racemiguembelina fructicosa				x			x	x																						
R. intermedia				x			x	x		x																				
Total counted (>63μm)	134	153	182	124	160	183	193	229	259	110	121	165	188	140	96	158	88	127	130	148	122	123	107	113	82	63	78	102	145	

Biozone	CF3																														
Core section	29-2	29-2	30-1	30-2	30-2	30-3	30-4	30-5	31-1	31-2	31-3	31-4	31-5	32-1	32-2	32-3	32-4	32-5	32-6	33-1	33-2	34-1	34-2	34-3	34-4	35-2	35-3	36-1	36-2
Interval (cm)	80	100	54	48	140	94	100	139	111	140	140	96	98	100	99	97	99	96	96	99	102	97	98	99	101	100	100	100	100
Globigerinelloides aspera	x	2.2	4	1	15.8	9.3	11	6	7.5	2.5	3.6		4	1		1	1				1	6	1	1				8	3
G. yaucoensis																													
Globotruncanella havanensis																													
G. petaloidea																													
G. subcarinatus																													
Hedbergella holmdelensis																													
H. monmouthensis	1.2	3	5.6	5.3	1.5	6.7	18	4.5	1.5	1	4.8	6	5	x	2	5	7	5	3		1	4	5	4					
Rugoglobigerina rugosa	3.7	x	3.2	4	3.3	12	11	3	1.5	1.7	1	1	1	1	2	1	3	3			3	1	1	2				63	57
Heterohelix globulosa	7.4	9.6	4.8	1	25.8	8.3	21	12	13	10	8.5	7	3	x		1	2											19	20
H. dentata	12.3	6.6	4.8	3.5	22.6	37	16	20	17	12	4.8	7	34	13	5	8	7	4	7	8	13	20	12	6	x	x	x	8	20
H. planata										1																			
H. navarroensis	8	2.2	1		1	1		1.5	1.5	1.7	3.6	4		3	3														
P. cf costulata		1.4			2.5				6.7	4.2	4.8				2														
Guembelitria cretacea	58.6	59	60.4	77	11			42	44	52	67	75	53	56	72	73	74	75	79	73	74	60	60	67	x	x	x		
Guembelitria dammula	4.3	14	6.4	7					4.5	6	1			17	9	9	6	13	11	19	7	9	17	10	x	x	x		
Zeauvigerina waiparaensis	2.4	1.4	9.6		5	20	24	9.8	4.5	6	1			7	5						1		4	10				2	
Gublerina robusta																													
P. deformis (=P. elegans)																													
P. hariaensis																													
P. palpebra																													
P. carseyae																													
A. cretacea																													
Globotruncana aegyptiaca																													
G. arca																													
G. rosetta																													
G. insignis																													
G. contusa																													
G. stuarti																													
G. pettersi																													
G. conica																													
Abathomphalus mayaroensis																													
Racemiguembelina fructicosa																													
R. intermedia																													
Total counted (>63μm)	162	135	124	168	120	120	38	132	133	118	82	132	131	258	148	276	197	159	120	32	157	162	100	112	0	0	0	90	48

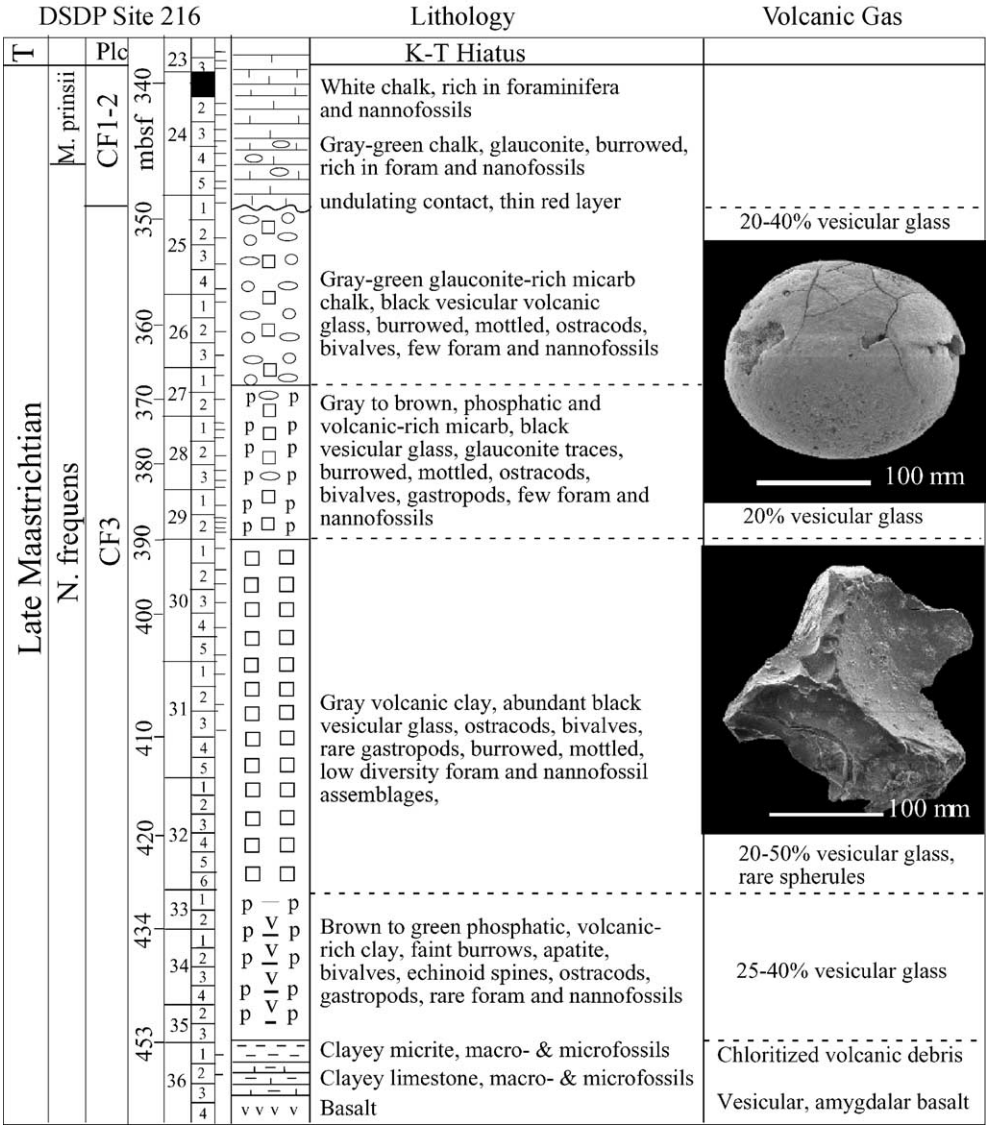

Fig. 2. Lithologic column, description, and volcanic input of DSDP Site 216. Note that black and brown vesicular volcanic glass is abundant, although variable in the various lithologic units. Volcanic spherules are rare.

Overlying this unit is a brown to green phosphatic and volcanic-rich clay (cores 32–35) that is burrowed and contains phosphate, apatite, basalt, and abundant glass (25–40%; Von der Borch et al., 1974). Macrofossils are common, including bivalves, ostracods, echinoid spines, and rare gastropods. Hekinian (1974) suggested that the volcanic debris may be eroded from the underlying older volcanic deposits, or may represent ejecta from the last stage of volcanism. Unusually high-stress microfossil assemblages in these sediments suggest the latter (discussed below).

Gray volcanic clay with abundant black vesicular glass (20–50%) characterizes cores 30–32 (Fig. 2). This interval is burrowed, mottled, and contains oysters, bivalve shells, ostracods, rare gastropods, and very low diversity assemblages of benthic and planktic foraminifera. The transition from this volcanic clay unit to the overlying green-to-brown

phosphatic and volcanic-rich micarb (micritic carbonate with silt-sized carbonate particles) occurs in core 29, although core recovery is incomplete. The phosphatic unit spans cores 27-1 to 29-2 and contains common brown-to-black vesicular glass (20%) and traces of glauconite, particularly in cores 28-3 and 27-2 (Fig. 2). The unit is generally burrowed and mottled and contains common oyster shells and bivalve fragments, rare gastropods, and few to rare benthic and planktic foraminifera and nannofossils.

The phosphatic unit grades into gray-green glauconite-rich micarb chalk (cores 27-1 to 25-1) that contains abundant brown-to-black vesicular glass (20–40%), common oyster shells and bivalve fragments, and few to rare foraminifera. The transition to the overlying chalk unit occurs in the upper part of core 25-1 (50 cm) and is marked by a thin red layer (1–2 mm) and an undulating erosive contact with the overlying light gray chalk (Fig. 2).

The lowermost part of the chalk unit (cores 25-1 to 24-5) is light gray, mottled and burrowed with trace amounts of glauconite, and contains abundant foraminifera and nannofossils, but no macrofossils. Above this interval is a gray-green laminated, glauconite-rich chalk (cores 24-4 to 24-5) that is mottled and burrowed. The upper part of the chalk unit analyzed (core 23) is white and rich in foraminifera and nannofossils. The K–T boundary was identified between core 23-3 (140 cm) and 23-3 (98 cm), and marks a major hiatus (see Section 4).

4. Biostratigraphy

4.1. K–T boundary

Previous studies placed the K–T boundary in core 23-2 between 100 and 120 cm based on the last occurrence of the nannofossil *Nephrolithus frequens* at 120 cm (Gartner, 1974) and the first appearance of Danian planktic foraminifera at 106 cm (McGowran, 1974). Most Cretaceous nannofossils are reported to disappear between cores 23-3 and the base of core 23-2, and no "typical Danian elements" of planktic foraminifera are reported to occur below core 23-2 (100 cm). McGowran (1974) thus estimated a K–T hiatus spanning from the late Maastrichtian (*Abathomphalus mayaroensis* zone) to the early Paleocene zone Pld.

In this study, the K–T boundary is placed in core 23-3 between 98 and 140 cm based on the first appearance of Danian planktic foraminifera at 98 cm. At this level, the first Danian assemblage contains zone Plc species, including *Parasubbotina pseudobulloides*, *Subbotina triloculinoides*, and *Morozovella inconstans*, mixed with abundant reworked late Maastrichtian species, which are also present in the mottled and bioturbated interval above (sections 23-3 and 23-2). This suggests a hiatus from Plc to the late Maastrichtian upper zone CF1, or about 2 myr. The discrepancy between this and the earlier study is likely due to the larger size fraction analyzed by McGowran (1974), which would not have recorded the earlier smaller Danian species.

However, the presence of early Danian zone Plc in core 23-3 also suggests that the K–T boundary interval may be significantly more complete than was previously estimated, but not recovered during coring. This is evident by poor recovery in core 23 where the lower part (Sections 4–6) is missing as well as the top of core 24 (Section 1). Thus, an interval of at least 6 m spanning the latest Maastrichtian zone CF1 and early Danian is missing due to a coring gap.

4.2. Late Maastrichtian

The chalks below the K–T boundary contain planktic foraminiferal assemblages characteristic of zone CF1-2 and nannofossil assemblages of *Micula prinsii* zone (Fig. 2). (The zone CF1 tropical index species *Plummerita hantkeninoides* is absent in middle latitudes.) This indicates that deposition of the chalk interval above the disconformity in core 25-1 occurred sometime during the last 500 kyr of the Maastrichtian. The global sea level lowstand at 65.5 Ma corresponds with the disconformity and hiatus between the chalk and underlying volcanic-rich sediments. This sea level lowstand is associated with widespread erosion and has recently been observed in Madagascar, Israel, and Egypt (Abramovich et al., 2002; Keller, 2002, 2004).

In the volcanic-rich sediments below the disconformity, the impoverished planktic foraminiferal assemblages are difficult to date. We tentatively assign a zone CF3 based on correlation with similar assemblages in Madagascar and Egypt. Nannofossils indicate the *Nephrolithus frequens* zone (Gartner,

1974; Tantawy and Keller, 2003) correlative with the *Micula murus* zone in Madagascar and Egypt (Tantawy and Keller, 2003). The base of zone CF3 and *N. frequens* or *M. murus* zone is at about 66.6 Ma. The much younger K–Ar age of 64.1±1.0 Ma reported by McDougall (1974) based on a basalt sample from core 37 is likely compromised by argon loss. Volcanic influx ceased around 65.5 Ma, as indicated by the onset of limestone deposition in zones CF1-2 and *M. prinsii*. Site 216 was thus within the sphere of mantle plume volcanism for about 1.1 myr, assuming that the base of zones CF3 and *N. frequens* were recovered. Sediment accumulation for the volcanic-rich interval averaged at least 7.5 cm/1000 years due to very high volcanic input.

5. Benthic foraminifera: biotic effects and subsidence history

Benthic foraminifera are generally present throughout the section analyzed and their variations in diversity, species size, and composition reveal unusual environmental stresses related to mantle plume activity and lithospheric subsidence of Site 216 after passage over the mantle plume. Normal-sized species assemblages and oxic bottom water conditions appear only after volcanic influx ceases and normal sedimentation resumes in the white chalk unit below the K–T boundary (Fig. 3). Benthic assemblages thus trace the subsidence history and bottom water conditions of Site 216 in relation to Ninetyeast Ridge volcanism during the late Maastrichtian.

5.1. Ninetyeast Ridge built to islands or sea level

The first fossil assemblages appear in the clayey limestone of core 36-2 that overlies basement basalt. Benthic foraminifera, ostracods, bivalve fragments, echinoid spines, and gastropods are abundant, whereas planktic foraminifera are relatively few (~8%; Fig. 3). Both benthic and planktic foraminifera are of normal size (>150 μm) and morphology. Benthic diversity is very low (16 species) and dominated by *Anomalinoides newmanae* (30%), *Valvulinaria* (10%), *Epistominella minuta* (8.8%), and few to common *Bagatella coloradoensis*, *Alabamina midwayensis*, *Gyroidinoides girardanus*, *Bolivinoides midwayensis* (2–5%), *Praebulimina cushmani*, *Praebulimina carseyae*, *Nonionella* sp., *Lenticulina*, *Pullenia*, *Nodosaria*, *Globulina*, and *Lagena*. This assemblage is unusual in that it is dominated by shallow inner neritic species (e.g., *A. newmanae*, *B. coloradoensis*, *Nonionella* sp.), but includes abundant middle to outer neritic and upper bathyal dwellers. The abundance of shallow water species as well as ostracods, bivalves, gastropods, and echinoid spines indicates that deposition occurred in a well-oxygenated shallow inner neritic or subtidal environment with an influx of reworked foraminifera from older uplifted sediments. This supports the interpretation of Ninetyeast Ridge hills built to sea level or islands as the oceanic plate moved over the mantle plume (Thompson et al., 1974; Moore et al., 1974).

In the overlying clayey micrite (core 36-1), the macrofossil assemblage remains the same. The benthic species assemblage is similar, but much less abundant (about 1/4) and dominated by just one species, *A. newmanae* (77%), with all other species few to rare. This indicates that deposition continued in a shallow subtidal environment, but with reduced input of reworked benthic foraminifera, which may reflect the onset of subsidence. Similar low-diversity benthic assemblages dominated by *A. newmanae* have been observed from the late Maastrichtian at Brazos River, Texas (Keller, 1992). The near-absence of agglutinated tests and miliolids and the presence of invertebrate macrofossils suggest normal salinity.

5.2. Rapid subsidence

In the phosphatic volcanic-rich clay above the clayey micrite (core 35), only rare, poorly preserved, and apparently reworked bivalves, ostracods, and gastropods are present, and benthic and planktic foraminifera are very rare or absent. The generally

Fig. 3. Benthic foraminifera, benthic/planktic ratio, subsidence history, and inferred paleodepth of Site 216 associated with mantle plume volcanism. Note the rapid subsidence from subtidal to middle and outer neritic depth by the end of volcanic influx. The sharp drop to upper bathyal depth during the late Maastrichtian zones CF2-1 is due to subsidence plus a rising sea level associated with the late Maastrichtian warm event between 200–400 kyr before the K–T boundary (description of lithology in Fig. 2).

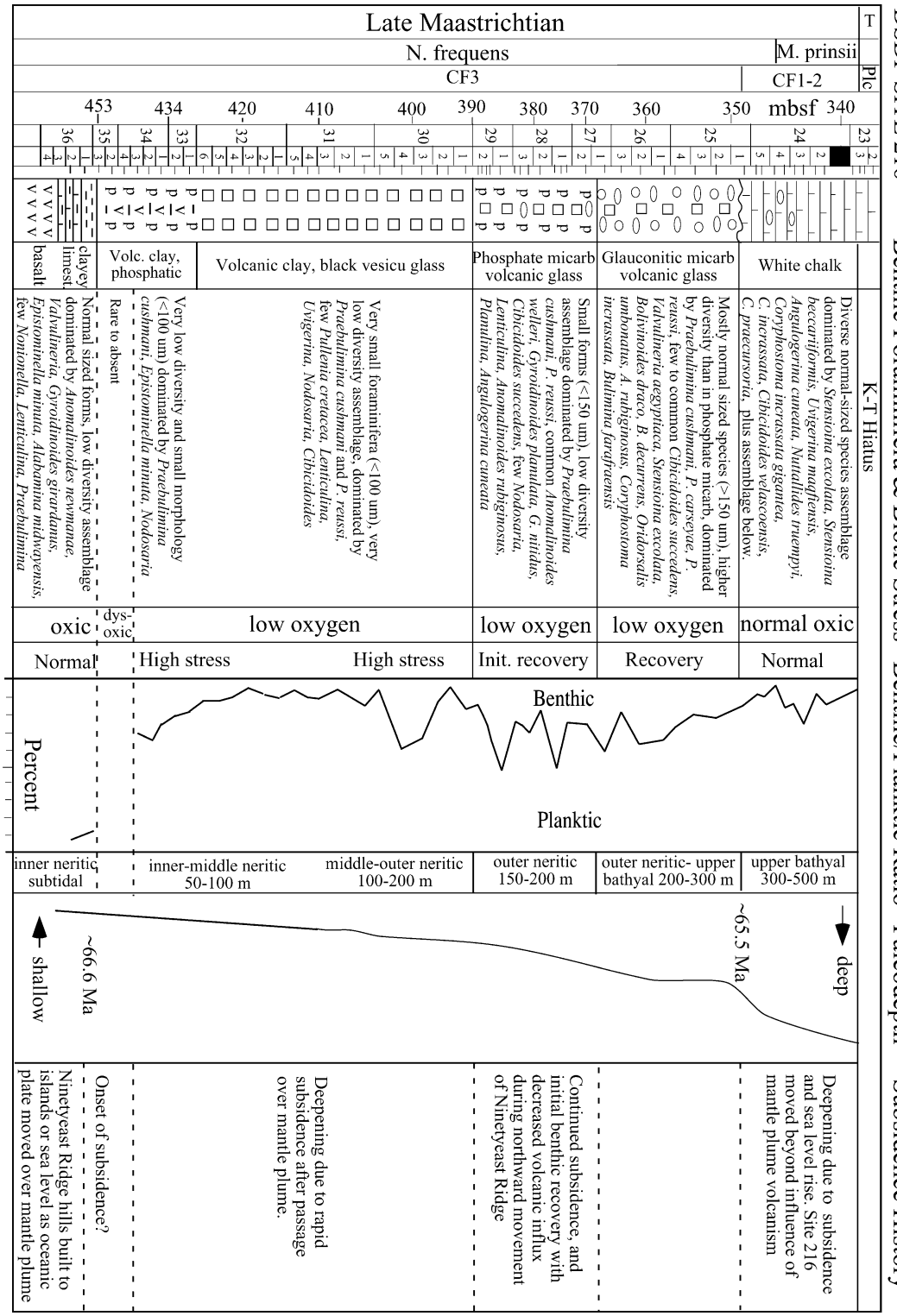
DSDP SITE 216
Benthic Foraminifera & Biotic Stress
Benthic/Planktic Ratio
Paleodepth
Subsidence History
Late Maastrichtian
N. frequens
M. prinsii
CF3
CF1-2
T
Plc
mbsf
K-T Hiatus
White chalk
Glauconitic micarb volcanic glass
Phosphate micarb volcanic glass
Volcanic clay, black vesicu glass
Volc. clay, phosphatic
clayey limest.
basalt
Diverse normal-sized species assemblage dominated by Stensioina excolata, Stensioina beccariiformis, Uvigerina mageshensis, Angulogerina cuneata, Nuttallides truempyi, Coryphostoma incrassata gigantea, C. incrassata, Cibicidoides velascoensis, C. praecursoria, plus assemblage below.
Mostly normal sized species (>150 um), higher diversity than in phosphate micarb, dominated by Praebulimina cushmani, P. carseyae, P. reussi, few to common Cibicidoides succedens, Valvulineria aegyptiaca, Stensioina excolata, Bolivinoides draco, B. decurrens, Oridorsalis umbonatus, A. rubiginosus, Coryphostoma incrassata, Bulimina farafraensis
Small forms (<150 um), low diversity assemblage dominated by Praebulimina cushmani, P. reussi, common Anomalinoides welleri, Gyroidinoides planulata, G. nitidus, Cibicidoides succedens, few Nodosaria, Lenticulina, Anomalinoides rubiginosus, Planulina, Angulogerina cuneata
Very small foraminifera (<100 um), very low diversity assemblage, dominated by Praebulimina cushmani and P. reussi, few Pullenia cretacea, Lenticulina, Uvigerina, Nodosaria, Cibicidoides
Very low diversity and small morphology (<100 um) dominated by Praebulimina cushmani, Episotominella minuta, Nodosaria
Rare to absent
Normal sized forms, low diversity assemblage dominated by Anomalinoides newmanae, Valvulineria, Gyroidinoides girardanus, Epistominella minuta, Alabamina midwayensis, few Nonionella, Lenticulina, Praebulimina
upper bathyal 300-500 m
outer neritic- upper bathyal 200-300 m
outer neritic 150-200 m
middle-outer neritic 100-200 m
inner-middle neritic 50-100 m
inner neritic subtidal
normal oxic
low oxygen
low oxygen
low oxygen
dys-oxic
oxic
Normal
Recovery
Init. recovery
High stress
High stress
Normal
Benthic
Planktic
Percent
0
50
100
deep
shallow
~65.5 Ma
~66.6 Ma
Deepening due to subsidence and sea level rise. Site 216 moved beyond influence of mantle plume volcanism
Continued subsidence, and initial benthic recovery with decreased volcanic influx during northward movement of Ninetyeast Ridge
Deepening due to rapid subsidence after passage over mantle plume.
Onset of subsidence?
Ninetyeast Ridge hills built to islands or sea level as oceanic plate moved over mantle plume

barren character of these sediments may be due to high nutrient influx, as suggested by the presence of phosphate and apatite, and consequently dysoxic conditions. In the similar sediments above this interval (cores 34 and 33), benthic (and planktic) foraminifera are tiny (<100 μm) with benthic assemblages dominated by *P. cushmani* and *E. minuta*, with few *Pullenia*, *Bolivinoides*, and *Nodosaria*, suggesting a high-stress low-oxygen environment. The generally deeper inner to middle neritic character of this assemblage and high benthic/planktic ratio (70–85% planktics) indicate rapid subsidence and a deepening environment (50–100 m; Fig. 3) after passage over the mantle plume.

Similarly, high-stress low-oxygen conditions prevailed in the overlying unit of volcanic clay with abundant vesicular black glass (20–50%). In this interval (cores 32–30), benthic species account for 10–15% of the total benthic and planktic assemblages and are dominated by *P. cushmani* and *P. reussi*, with few *Pullenia*, *Lenticulina*, *Uvigerina*, and *Cibicidoides*, which indicate further deepening to a middle–outer neritic environment (100–200 m; Von Morkhoven et al., 1986). Reworking and transport of species appear to have been minimal, or restricted to short distances, as suggested by the generally good preservation of foraminiferal shells. However, the predominantly small size and low species diversity indicate high-stress conditions due to low oxygen, a restricted environment, and ongoing volcanic activity. This is also suggested by the infaunal habitat of all but two morphotypes (*Lenticulina* and *Cibicidoides*) and low oxygen tolerance of all (Keller, 1992; Culver, 2003). Ostracods, bivalve shells, and rare gastropods are present. These benthic assemblages indicate further deepening due to continued subsidence (Fig. 3).

5.3. Continued subsidence and onset of biotic recovery

In the phosphatic–volcanic micarb (micritic carbonate) unit of cores 29 to 27-1 (Fig. 3), benthic foraminifera are slightly larger, more diverse, and abundant, but still unusually small (<150 μm) and of low overall diversity. Low-oxygen-tolerant species *Praebulimina cushmani* and *P. reussi* are still dominant, although *Anomalinoides welleri*, *Gyroidinoides nitidus*, *G. planulata*, and *Cibicidoides succedens* are common, and few *Nodosaria*, *Lenticulina*, *Planulina*, *Angulogerina cuneata*, and *Anomalinoides rubiginosus* are present. This assemblage indicates deposition in a deeper outer neritic (150–200 m) environment and the increase in epifaunal species (*Anomalinoides*, *Cibicidoides*, *Lenticulina*, *Planulina*, *Gyroidinoides*, and *Angulogerina*) suggests less restricted conditions. Benthics average 20–30% of the total foraminiferal assemblage in this interval apparently as a result of the low planktic abundance due to increased stress in surface waters (see below). Oyster and bivalve shells are present. These benthic assemblages indicate continued subsidence and the onset of benthic recovery as volcanic influx decreased with the northward movement of Ninetyeast Ridge.

In the glauconitic–volcanic micarb unit (cores 27-1 to 25-1), benthic species are mostly of normal size (>150μm) and higher diversity. Low-oxygen-tolerant praebuliminids (*P. cushmani*, *P. reussi*, and *P. carseyae*) still dominate along with few to common *C. succedens*, *Valvulineria aegyptiaca*, *Stensioina excolata*, *Bolivinoides draco*, *Bolivinoides decurrens*, *Coryphostoma incrassata*, *Anomalinoides rubiginosus*, *Bulimina farafraensis*, and *Oridorsalis umbonatus* (Fig. 3). Ostracods and bivalves are present. These assemblages indicate continued subsidence and deposition in a deeper outer neritic to upper bathyal environment (200–300 m). The return to normal species size and increased diversity in both infaunal (*Boliviodes*, *Coryphostoma*) and epifaunal species indicate the return to more normal, but still low-oxygen conditions on the ocean floor.

5.4. Rapid deepening and biotic recovery

In the white chalk unit (cores 25-1 to 23-3), benthic foraminiferal assemblages are diverse, of near-normal

Fig. 4. Relative percent abundances of planktic foraminiferal species (>63 μm) and species richness at Site 216. Note that the first species assemblages above basement basalt are reworked in a subtidal environment. Above this interval, the disaster opportunist *Guembelitria* dominates faunal assemblages, followed by low-oxygen-tolerant heterohelicids, although species richness is extremely low. As Site 216 moved beyond the influence of mantle plume volcanism, the appearance of more specialized species signals the return of more normal environmental conditions (description of lithology in Fig. 2).

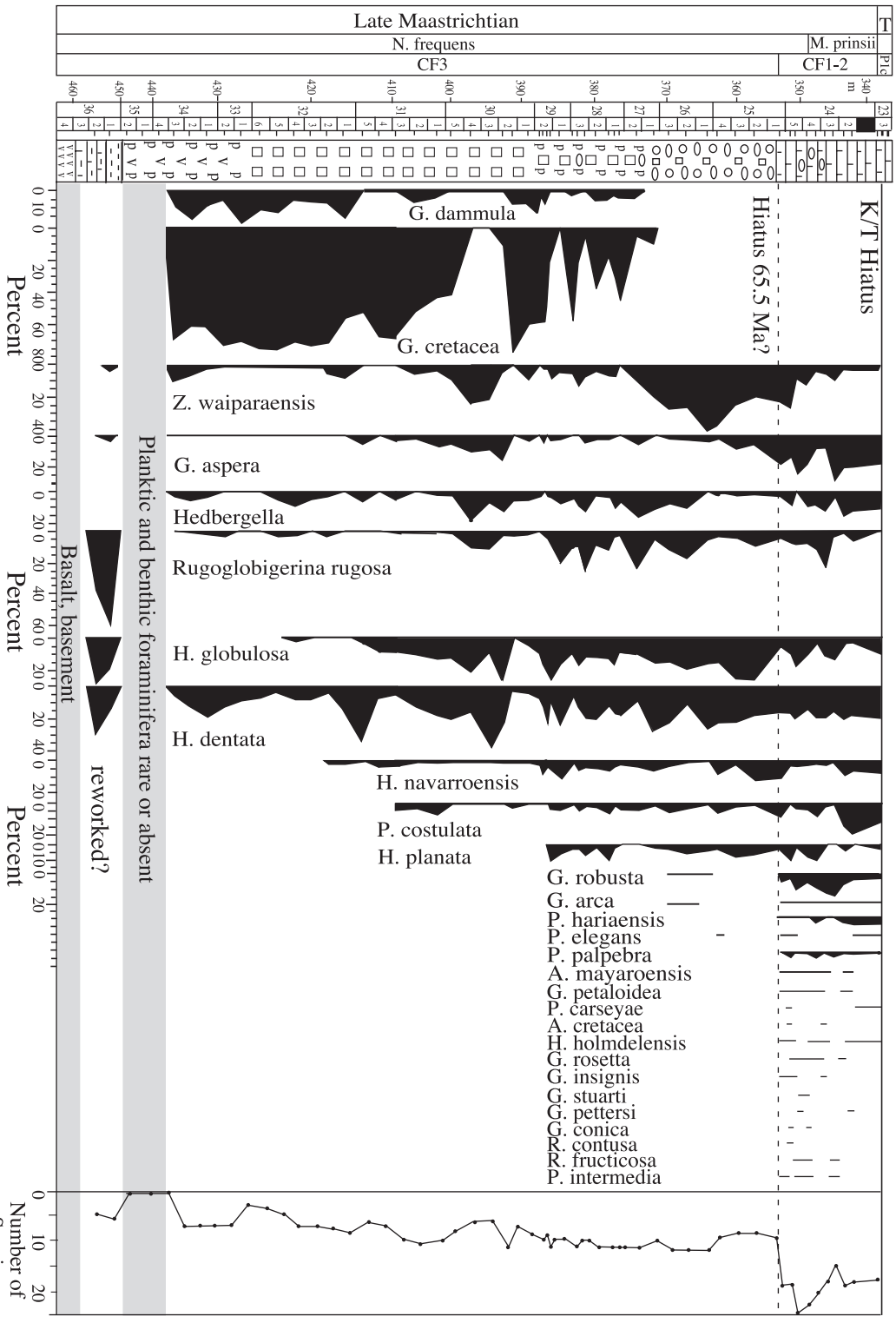
DSDP Site 216 Relative Percent Abundances of planktic Foraminifera (>63um) Species Richness
Late Maastrichtian
N. frequens
CF3
M. prinsii
CF1-2
K/T Hiatus
Hiatus 65.5 Ma?
G. dammula
G. cretacea
Z. waiparaensis
G. aspera
Hedbergella
Rugoglobigerina rugosa
H. globulosa
H. dentata
H. navarroensis
P. costulata
H. planata
G. robusta
G. arca
P. hariaensis
P. elegans
P. palpebra
A. mayaroensis
G. petaloidea
P. carseyae
A. cretacea
H. holmdelensis
G. rosetta
G. insignis
G. stuarti
G. pettersi
G. conica
R. contusa
R. fructicosa
P. intermedia
Planktic and benthic foraminifera rare or absent
reworked?
Basalt, basement
Percent
Number of Species

species size, and characterized by the appearance of predominantly upper bathyal species including *Stensioina beccariiformis*, *S. excolata*, *Uvigerina maqfiensis*, *Angulogerina cuneata*, *Nuttallides truempyi*, *C. incrassata gigantea*, *C. incrassata*, *Cibicidoides velascoensis*, and *C. praecursoria*, which indicate normal oxic bottom waters. Most species of the underlying glauconitic interval are still present, although in low abundances, but macrofossils are rare or absent. These assemblages are characteristic of deposition in a deeper upper bathyal environment below the photic zone (300–500 m; Fig. 3; Von Morkhoven et al., 1986) and under normal marine conditions. This is also indicated by a very low benthic/planktic ratio, the appearance of the first normal-sized planktic foraminifera, and increased species diversity (Figs. 3 and 4). The rapidly deepening depositional environment is likely due to continued lithospheric subsidence coupled with the late Maastrichtian sea level rise, particularly during the climate warming between 200 and 400 kyr before the K–T boundary (Li and Keller, 1998b; Li et al., 2000). The return of normal benthic and planktic assemblages signifies the return to more normal marine conditions as Site 216 moved beyond the influence of mantle plume volcanic activity during the late Maastrichtian zones CF1-2 and *M. prinsii* zone.

6. Planktic foraminifera: biotic effects of volcanism

Late Maastrichtian planktic foraminiferal assemblages in the volcanic-rich sediments at Site 216 are characterized by unusually low species richness (6–10 species), a 90% reduction in overall diversity, very small adult species sizes (<100 μm), and low abundances compared with assemblages at similar middle to high latitudes (~40°S), except for the unusually high abundances of the disaster opportunist *Guembelitria cretacea*. More diverse species assemblages with normal adult species sizes first appear in the chalk near the top of the section and above the volcanic-rich sediments (Fig. 4). Preservational effects cannot account for these unusual assemblages since foraminiferal tests are generally well preserved, with minor recrystallization and calcite infilling. Dissolution effects are minor (some breakage and holes in tests) as evident in the high abundance of small delicate species. These unusual high-stress assemblages appear to be directly related to the passage of the oceanic plate over a mantle plume and consequent volcanic activity.

6.1. First planktic assemblages reworked?

The clayey limestone and micrite (core sections 36-2 and 36-1) that overlie basement basalt contain the first sparse planktic foraminifera. The assemblages are dominated by *Rugoglobigerina rugosa* (57–63%), *Heterohelix globulosa* (20%), and *H. dentata* (8% and 20%) with rare *Globigerinelloides aspera* and *Zeauvigerina waiparaensis* (Fig. 4, Table 1). All planktic species are of normal adult sizes. Tests are recrystallized with chamber infillings and frequently broken due to mechanical transport. The low planktic diversity and abundance, coupled with high benthic diversity and abundance, suggest a restricted shallow water habitat and/or reworking (Fig. 3). In similarly shallow lagoonal to subtidal paleoenvironments, planktic assemblages tend to have much higher diversity (~20–30 species) dominated by *G. cretacea* and small biserial species (*H. globulosa*, *H. dentata*, *H. navarroensis*, and *Z. waiparaensis*) (Keller et al., 1993, 1998, 2002a,b). The unusual and poorly preserved assemblage at Site 216 suggests preferential preservation and reworking of the more robust *R. rugosa*. The absence of similar assemblages in the overlying sediments also suggests that the planktic foraminifera in core 36 are reworked.

6.2. High-stress assemblages

In the phosphatic and volcanic-rich clay of core 34-4 to core 35, planktic and benthic foraminifera are

Fig. 5. Paleoecology of planktic foraminiferal assemblages at DSDP Site 216 on Ninetyeast Ridge, Indian Ocean. Note the disaster opportunists *Guembelitria* species thrived during high-stress conditions when few other species survived. At times of ecosystem recovery (decreased volcanism), *Guembelitria* nearly disappeared and low-oxygen-tolerant small biserial species thrived along with common small planispiral and trochospiral surface dwellers (gray shaded intervals). Normal, more diverse faunal assemblages reappeared only after volcanism ceased, although species richness remained low (description of lithology in Fig. 2).

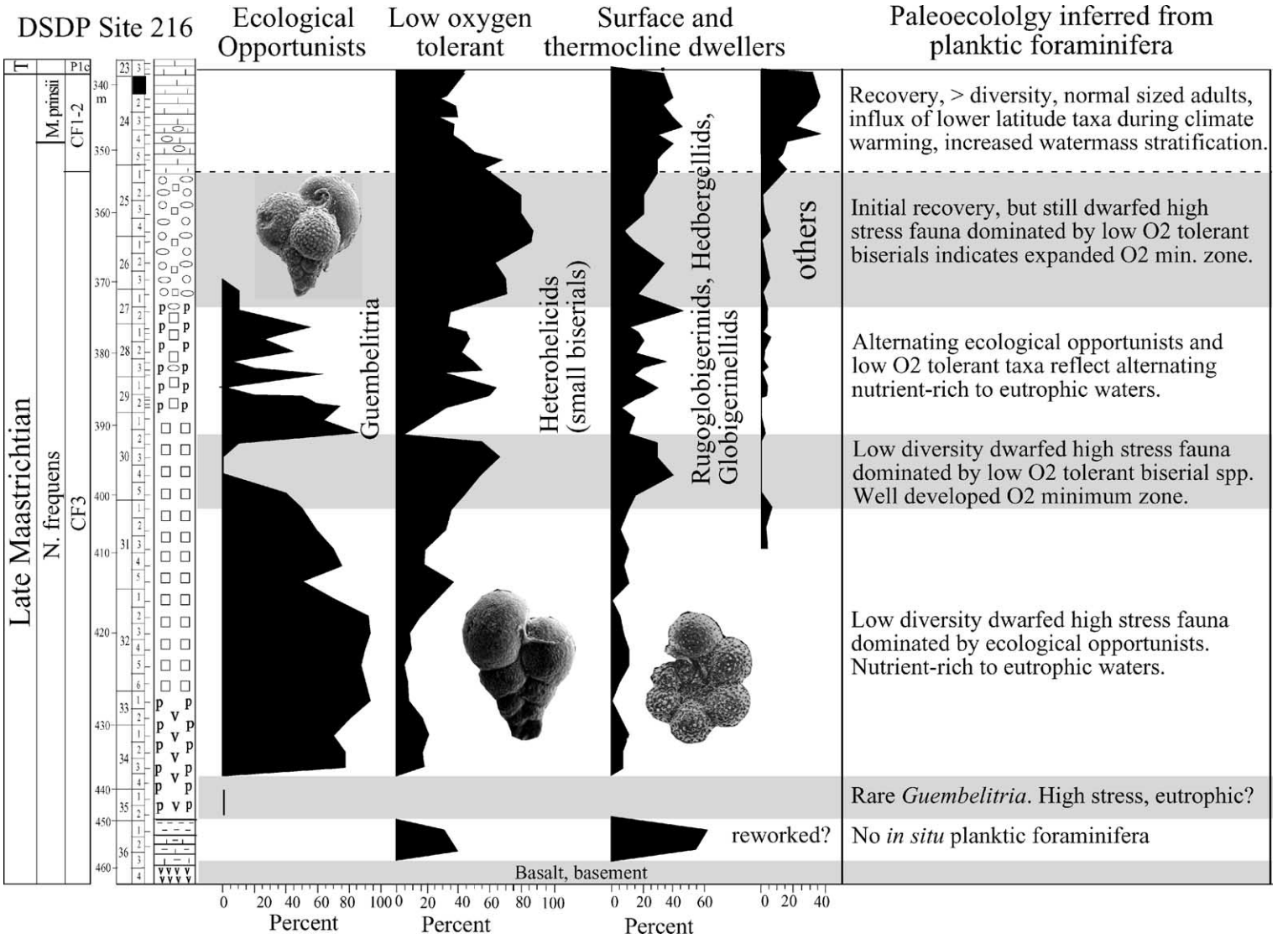
DSDP Site 216
Ecological Opportunists
Low oxygen tolerant
Surface and thermocline dwellers
Paleoecololgy inferred from planktic foraminifera
Late Maastrichtian
T
P1c
M. prinsii
N. frequens
CF1-2
CF3
m
Guembelitria
Heterohelicids (small biserials)
Rugoglobigerinids, Hedbergellids, Globigerinellids
others
Recovery, > diversity, normal sized adults, influx of lower latitude taxa during climate warming, increased watermass stratification.
Initial recovery, but still dwarfed high stress fauna dominated by low O2 tolerant biserials indicates expanded O2 min. zone.
Alternating ecological opportunists and low O2 tolerant taxa reflect alternating nutrient-rich to eutrophic waters.
Low diversity dwarfed high stress fauna dominated by low O2 tolerant biserial spp. Well developed O2 minimum zone.
Low diversity dwarfed high stress fauna dominated by ecological opportunists. Nutrient-rich to eutrophic waters.
Rare Guembelitria. High stress, eutrophic?
reworked?
No in situ planktic foraminifera
Basalt, basement
0 20 40 60 80 100
Percent
0 20 40 60 80 100
Percent
0 20 40 60
Percent
0 20 40

absent, except for very rare disaster opportunist *G. cretacea* (Keller et al., 2002a). This suggests inhospitable conditions related to volcanic influx. The first sparse planktic assemblages appear in cores 33 to 34-3 and consist of unusually impoverished high-stress assemblages dominated by tiny (<100 μm) adult *G. cretacea* (~60–80%) and *G. dammula*, small heterohelicids, and rare small *Rugoglobigerina rugosa* (Fig. 4). The same *Guembelitria*-dominated assemblage persists in the overlying volcanic clay and glass unit of cores 31–32, where the combined abundance of *Guembelitria* species reaches a maximum of 90% and species diversity is at its lowest (three to seven species; Figs. 4 and 5). The presence of phosphate and apatite suggests that high-stress conditions may be largely due to eutrophic waters.

The assemblage dramatically changes in cores 30-2 to 30-4 where *Guembelitria* is nearly absent, but low-oxygen-tolerant biserial species dominate (60% combined abundance of *H. globulosa*, *H. navarroensis*, *H. dentata*, and *Z. waiparaensis*) and surface dwellers *R. rugosa*, *Hedbergella* sp., and *G. aspera* are common (maximum 40%). This suggests increased watermass stratification and development of an oxygen minimum zone (Figs. 4 and 5).

In the phosphatic, glauconitic, and volcanic-rich micritic carbonate of cores 27–29, species diversity is slightly higher (11 species), including an increasing abundance of surface dwellers (e.g., *Rugoglobigerina*, *Pseudoguembelina costulata*). Ecological opportunist *Guembelitria* and low-oxygen-tolerant heterohelicids alternate in this interval. This suggests alternating nutrient-rich to eutrophic surface waters and a well-developed oxygen minimum zone (Fig. 5). All adult species are still extremely small (<100 μm), indicating that high-stress conditions continued.

6.3. Onset of biotic recovery

Similar dwarfed species assemblages are present in the glass and glauconite-rich micritic chalk of cores 25 and 26, except that *Guembelitria* are absent (Fig. 4). The assemblage is dominated by low-oxygen-tolerant small heterohelicids, which reach a maximum of 80% (Figs. 4 and 5). There are rare occurrences of *Gublerina robusta*, *Globotruncana arca*, and *Pseudotextularia elegans*. This suggests an expanded oxygen minimum zone, increased surface productivity, and increased watermass stratification (Fig. 5). The disappearance of *Guembelitria* is likely due to increasing competition (e.g., *Rugoglobigerina*, *P. costulata*, and *G. aspera*), but also reflects initial biotic recovery of Site 216. The reduced species sizes (<100 μm), however, indicate continued high-stress conditions.

Only in the gray-green and white chalks of cores 24 to 25-1 do planktic foraminiferal assemblages reach more normal adult sizes (>150 μm), indicating recovery of the pelagic environment. This is also indicated by the absence of *Guembelitria* opportunists, decreased abundance of low O_2-tolerant heterohelicids, increased abundance of small surface dwelling generalists, and increase in large subsurface or thermocline dwellers (Fig. 5). This indicates the return of normal marine productivity and watermass stratification. Although species richness increased to an average of 17 species, it remained well below normal diversity (30–40 species) for equivalent latitudes (e.g., Site 525; Li and Keller, 1998a; Abramovich and Keller, 2003). A short-term influx of species from lower latitudes (e.g., globotruncanids, gublerinids, racemiguembelinids, and pseudotextularids) temporarily raised species richness to 25 and likely reflects the climate warming between 200 and 400 kyr before the K–T boundary (Li and Keller, 1998b; Kucera and Malmgren, 1998). Stress-tolerant species continue to dominate faunal assemblages.

The absence of a transitional character between the dwarfed high-stress assemblages of the volcanic-rich sediments and more normal-sized assemblages of the overlying chalk is due to a hiatus at the CF1-2/CF3 transition. A major hiatus also marks the K–T boundary where Danian zone Plc (core 23-3; 98 cm) overlies upper Maastrichtian sediments (core 23-3; 140 cm) and spans the basal 500 kyr of the Danian (zones P0, Pla, and Plb) and part of the uppermost Maastrichtian. For this reason, no direct comparison can be made with the K–T mass extinction at Site 216.

7. Planktic foraminifera—paleoecologic proxies

Relative species abundances at Site 216 thus reveal that different lithological units are associated with distinct dominant species populations that reflect environmental changes (Fig. 5). Moreover, there is a

progressive change from maximum stress conditions near the base of the volcanic phosphate and apatite-rich unit to steadily improving and less stressful conditions towards the top of the volcanic-rich units. The degree of biotic stress and ecological conditions can be inferred from various ecologic proxies, including species size and morphology, type of species, abundance, and species richness or diversity.

7.1. High-stress proxy—dwarfism

Dwarfing of species is commonly observed across the K–T transition in shallow or deep waters and across latitudes (e.g., Brazos, Texas, DSDP Site 738 in the South Atlantic, Egypt, Israel, Tunisia; Keller, 1989, 1993; MacLeod et al., 2000; Keller et al., 1998), and has recently been documented from late Maastrichtian sediments of Israel, Egypt, Madagascar, and South Atlantic Site 525 (Abramovich et al., 1998, 2002; Abramovich and Keller, 2003; Keller, 2002, 2003). At Site 525, dwarfing also affected ecological specialist species, particularly during the late Maastrichtian warm event (65.4–65.2 Ma). Dwarfing has also been observed in calcareous nannofossil assemblages of low and middle latitudes (Gardin and Monechi, 1998; Tantawy, 2002, 2003; Tantawy and Keller, 2003). In general, the degree of dwarfing and relative species abundance is proportional to the environmental stress. But in none of the sections documented to date has the degree of dwarfing and reduced diversity equaled that of Site 216.

McGowran (1974, p. 625) suggested that these tiny foraminifera in Site 216 are "undoubtedly size-fractionated," implying that these assemblages may be size-sorted due to current winnowing. Size sorting—the preferential accumulation of small juvenile specimens—is not an option for two major reasons. First, in over 50 m of sediments representing variable depositional environments (volcanic, phosphatic, and glauconitic) and steadily deepening paleodepths, the assumption of constant current winnowing over several hundred thousand years cannot be supported. Current winnowing usually occurs in selected short intervals (due to intensified current circulation) and is not 100% effective in removing all larger-sized specimens, as is the case at Site 216, nor can it account for the observed species population trend. The complete absence of larger morphologies, even as broken fragments, indicates that larger morphologies did not inhabit this environment. Second, although the specimens are very small (63–100 μm), they are fully developed adults, as indicated by overall morphology, ratio of chamber development, and adult number of chambers. Juvenile forms are present in the smaller size fraction (38–63 μm). Similarly dwarfed species assemblages are well known from the K–T boundary (Keller, 1993; MacLeod et al., 2000; Keller et al., 2002a). At Site 216 on Ninetyeast Ridge, these unusual high-stress assemblages appear to be directly related to the passage of the oceanic plate over a mantle plume and consequent volcanic activity.

Extremely small adult size is characteristic of all species within the volcanic-rich Late Maastrichtian sediments of Site 216. In all planktic foraminiferal assemblages, species are tiny (<100 μm) and often less than half to one fourth their normal adult species size, yet fully adult, as indicated by the number of chambers, fully developed apertures, and surface ornamentation (MacLeod et al., 2000). They are therefore dwarfed species, rather than juveniles, where dwarfing is a function of high-stress conditions induced by the environment. These dwarfed species populations are present in shallow waters near the base of the section, as well as in the deeper waters, and can therefore not be explained by either shallow water or restricted conditions, but rather reflect adverse water-mass properties (e.g., nutrients, salinity, and oxygen), the nature of which still has to be determined.

7.2. High-stress proxy—low species richness

Low species richness (the number of species present) is another biotic stress proxy. In modern environments, the number and type of species in a given species pool are related to the environment (Murray, 2003). Similarly, fossil assemblages reflect the species pool of past environments. In shallow restricted environments, species richness is relatively low, ranging from 35 to 42 species in low latitudes (e.g., Brazos River, Texas, and Seldja in southern Tunisia; Keller, 1989; Keller et al., 1998) to less than 20 species in higher latitudes depending on paleodepth and stress conditions (e.g., Stevns Klint and Nye Klov, Danemark; Schmitz et al., 1992; Keller et al., 1993). But in normal marine environments during

the late Maastrichtian, planktic foraminiferal species richness is at a maximum (~65 species; e.g., Tethys Ocean) in well-stratified waters of open marine environments of low latitudes, decreases in middle latitudes (50–55 species, Site 525, Madagascar; Li and Keller, 1998a; Abramovich et al., 2002; Abramovich and Keller, 2003), and is strongly reduced in high latitudes (20–25 species, Site 738; Keller, 1993). Hence, open ocean assemblages at similar midlatitude localities as Site 216 (e.g., Site 525, Madagascar) are typically very diverse with between 50 and 55 species. The low species diversity and dwarfism at Site 216, with 3–11 species during volcanic input and 17–25 species after volcanic influx, ceased to reflect extreme biotic stress conditions and the delayed recovery during the last 400 kyr of the Maastrichtian (zones CF1-2, *M. prinsii*).

7.3. Ecological opportunists—disaster proxy *Guembelitria*

Guembelitria species are well-known ecological opportunists or disaster species that thrived in the most stressful habitats where few other species survived. For example, after the K–T mass extinction, *G. cretacea* is the only survivor species that thrived (see review in Keller et al., 2002a). Curiously, *G. cretacea* is also the most dominant species during the most intense volcanic influx when few other species survived at Site 216 (Fig. 5). These *G. cretacea*-dominated assemblages, associated with the phosphate- and glass-rich sediments, are almost identical to those in the early Danian after the K–T impact event. Within the interval of cores 31–35, the relative abundance of *Guembelitria* varies between 80% and 100%, with the remainder small heterohelicids and hedbergellids (Fig. 5). The same species with similar abundance proportions survived the K–T mass extinction in middle to low latitudes (review in Keller, 2001). The only significant difference in the early Danian is the evolution of the first Tertiary species. By comparison, the late Maastrichtian mantle plume volcanic activity on Ninetyeast Ridge locally created similarly high-stress conditions as the K–T event on a more global scale. *Guembelitria* dominance is thus a proxy for ecologic disasters, whether related to impact or volcanism.

There is evidence that late Maastrichtian biotic effects of volcanism in the Indian Ocean (either from the Ninetyeast Ridge and/or Reunion hotspots) are widespread, although probably not global. Opportunistic blooms of *Guembelitria* have now been documented from the late Maastrichtian at Bjala, Bulgaria (Adatte et al., 2002), Madagascar (Abramovich et al., 2002), central Egypt (Keller, 2002), and the Negev (Abramovich et al., 1998; Keller, 2003,2004) (Fig. 6). In these regions, *Guembelitria* blooms are associated with widely differing environments ranging from restricted basins to open marine, near shore to open ocean, shallow to deep waters, but always with high nutrient influx and low primary productivity. In post-K–T environments, the most intense *Guembelitria* blooms are associated in shallow marginal seas and continental margins. What all environments appear to have in common are nutrient-rich surface waters due to high nutrient influx from continental runoff, upwelling, or volcanic input (Fig. 7). Kroon and Nederbragt (1990) observed that in the modern ocean, low-diversity assemblages with common *Guembelitria* are associated with upwelling areas off the tip of southern India.

Guembelitria generally disappeared when environmental conditions sufficiently improved for competing surface dwellers to thrive. *Guembelitria* blooms thus resemble today's red tide algal blooms that occur in highly nutrient-rich or eutrophic waters as a result of influx from agricultural fertilizers. At Site 216, volcanic sediments provided the nutrient influx as evident in the high Ba, K, Ca, and Fe concentrations (Meudt et al., 2003), phosphate, apatite, and glauconite-rich sediments. Similarly elevated trace elements and increased nutrient flux are observed in association with igneous provinces near the Cenomanian–Turonian boundary (Kerr, 1998). With the first abatement

Fig. 6. Westward decrease of the disaster opportunist *Guembelitria* species from Site 216, Madagascar, Israel, Egypt, and Tunisia. Correlation is based on planktic foraminiferal biozones (dashed lines) and initial recovery intervals (gray shaded). Disaster and recovery intervals are summarized for comparison with periods of intense volcanic activity at Site 216, Deccan Traps (Hoffmann et al., 2000), and multiple impact events during the late Maastrichtian, K–T, and early Danian. Note that all periods of intense volcanism correspond with disaster opportunists, but not all impact events do.

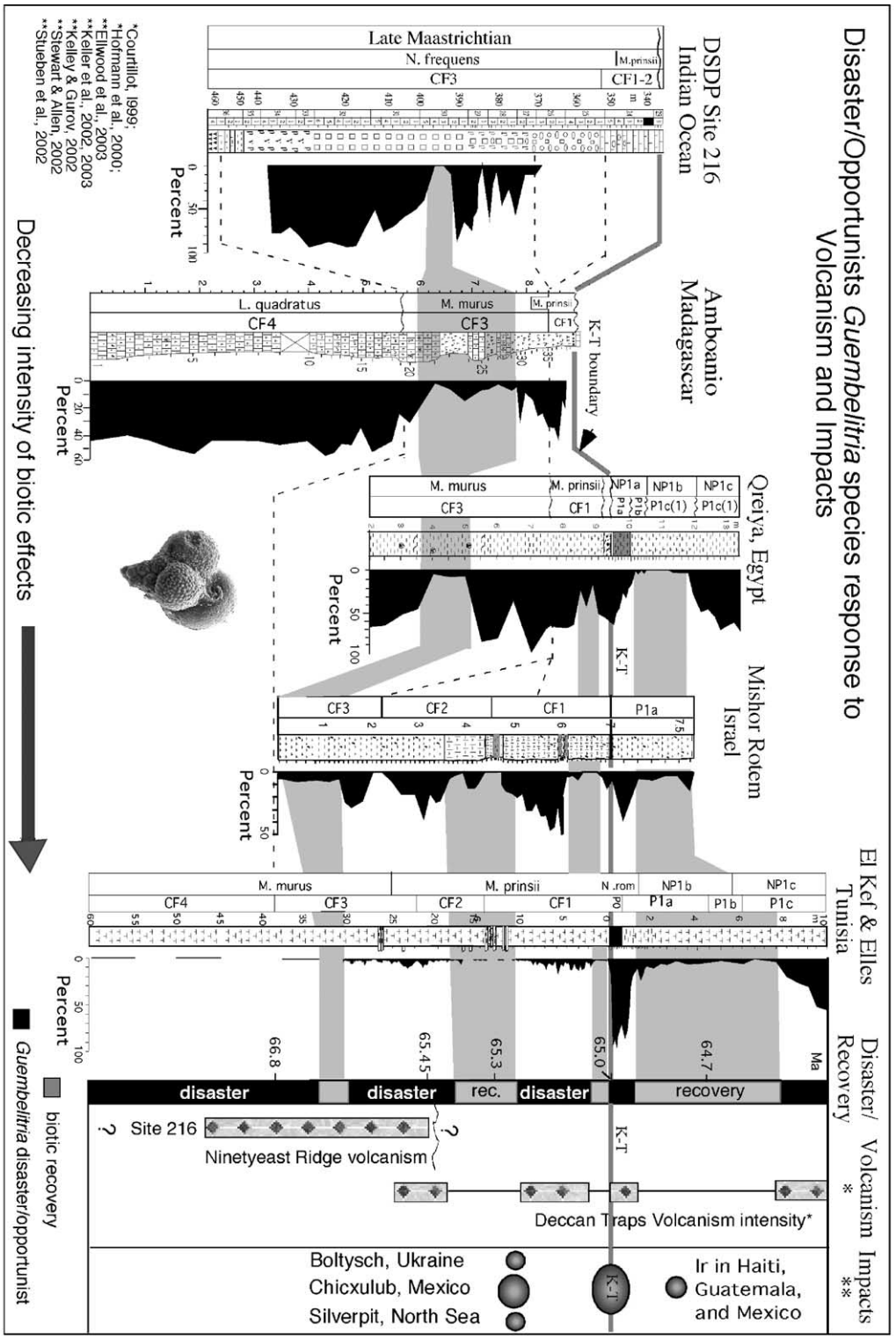
Disaster/Opportunists Guembelitria species response to Volcanism and Impacts
DSDP Site 216 Indian Ocean
Amboanio Madagascar
Qreiya, Egypt
Mishor Rotem Israel
El Kef & Elles Tunisia
Late Maastrichtian
N. frequens
M.prinsii
CF3
CF1-2
L. quadratus
M. murus
M. prinsii
CF4
CF3
CF1
K-T boundary
M. murus
M. prinsii
NP1a
NP1b
NP1c
CF3
CF1
P1c(1)
CF3
CF2
CF1
P1a
M. murus
M. prinsii
N .rom
NP1b
NP1c
CF4
CF3
CF2
CF1
P1a
P1b
P1c
Percent
K-T
66.8
65.45
65.3
65.0
64.7
Ma
disaster
disaster
rec.
disaster
recovery
Disaster/ Recovery
Volcanism *
Impacts **
? Site 216 ?
Ninetyeast Ridge volcanism
Deccan Traps Volcanism intensity*
Boltysch, Ukraine
Chicxulub, Mexico
Silverpit, North Sea
K-T
Ir in Haiti, Guatemala, and Mexico
Decreasing intensity of biotic effects
Guembelitria disaster/opportunist
biotic recovery
*Courtillot, 1999;
*Hofmann et al., 2000;
**Ellwood et al., 2003
**Keller et al., 2002, 2003
**Kelley & Gurov, 2002
**Stewart & Allen, 2002
**Stueben et al., 2002

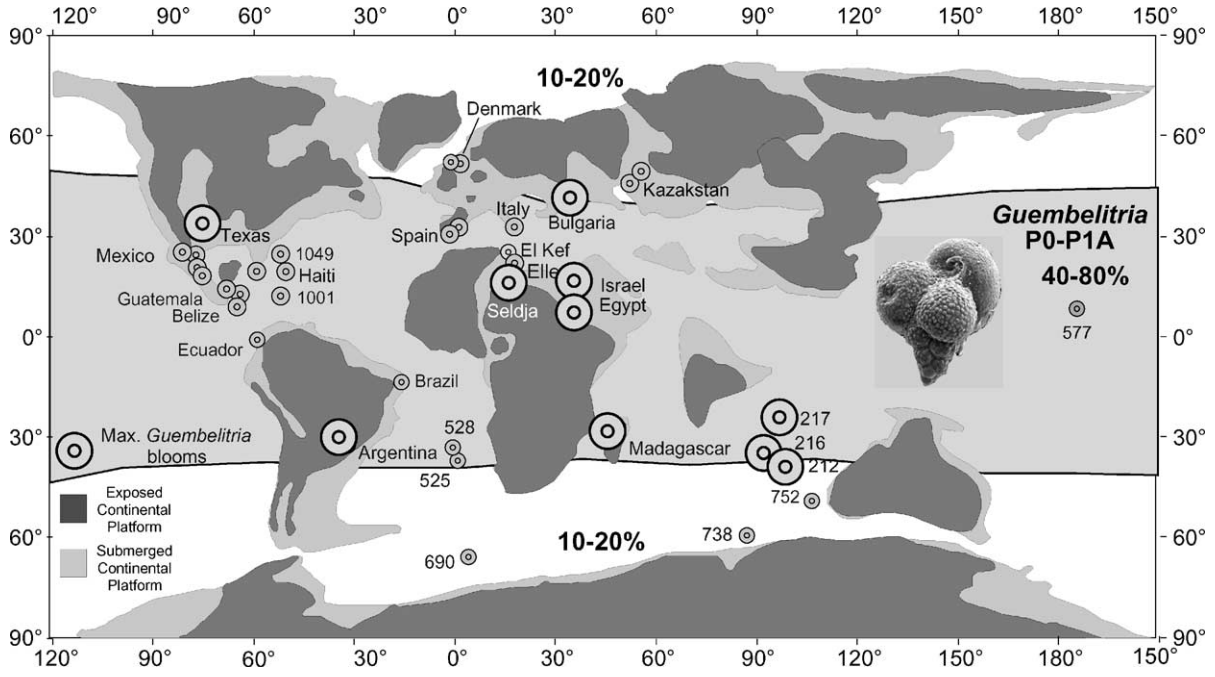

Fig. 7. Biogeographic distribution of *Guembelitria* blooms during the early Danian. Although these blooms occur worldwide, they are most intense in low to middle latitudes with *Guembelitria* populations comprising 40–80% of assemblages, as compared with 10–20% in high latitudes. This reflects the diminished biotic effects of the K–T catastrophe into higher latitudes. Note that the most intense *Guembelitria* blooms are found in shallow continental seas, continental margins, and volcanic provinces. What these environments have in common are high nutrient influx either due to terrestrial runoff, upwelling, or volcanic input.

of stress conditions, the disaster/opportunists give way to small ecological generalists in surface waters and the oxygen minimum zone.

7.4. Small heterohelicids—low O_2 proxy

Ecological generalists include a group of small biserial heterohelicids and trochospiral and planispiral globigerinellids and hedbergellids with nearly global paleogeographic range (Nederbragt, 1991,1992; Keller et al., 2002a). Among these species, heterohelicids tend to dominate at times when *Guembelitria* decrease or disappear (Fig. 5). Small heterohelicids (e.g., *H. globulosa*, *H. dentata*, *H. navarroensis*, and *Z. waiparaensis*) lived in surface to subsurface depths and tolerated low oxygen concentrations. High abundances of these species are generally associated with high surface productivity (high positive $\delta^{13}C$ values) and expanded oxygen minimum zones and are thus proxies for low O_2 conditions (e.g., Keller et al., 2002a).

For example, at Site 738 in the South Atlantic, *Z. waiparaensis* dominates at times of high positive $\delta^{13}C$ values and high Ba content (Keller, 1993; Barrera and Keller, 1994). The presence of a well-developed oxygen minimum zone also implies a well-stratified watermass, and hence more ecological niches and higher diversity of species. This is the case at Site 216 where dominant heterohelicids are associated with increased abundance of surface and near-surface dwellers (e.g., rugoglobigerinids, globigerinellids, and hedbergellids) and the absence of guembelitrids (Fig. 5). In this environment, guembelitrids are outcompeted by ecological generalists that thrived in ecological niches supplied by increased water mass stratification. This is particularly apparent in the glauconite and volcanic glass-rich interval of cores 25 and 26, and the volcanic glass-rich interval of cores 30-2 to 30-4. However, in the phosphate- and volcanic-rich interval of cores 27–29, ecological opportunists and generalists alternate, suggesting rapidly changing stress conditions.

7.5. Ecological specialists

In a well-stratified ocean with normal (low) nutrient flux, species diversity is generally at a maximum and species are large with complex morphologies. However, they tend to have restricted paleogeographic ranges and narrow tolerance limits for temperature, salinity, oxygen, and nutrients (Nederbragt, 1998; Keller et al., 2002a; Abramovich and Keller, 2003; Abramovich et al., 2003). For these reasons, they are the first to go in a stressed environment. At Site 216, near-normal species size and higher species richness are established during chalk deposition, after volcanic influx ceased near the base of zones CF1-2, or *M. prinsii* zone, about 300–400 kyr before the K–T boundary. Diversity in this interval averages 17 species with a maximum of 25 species due to a short-term influx of lower-latitude species (e.g., globotruncanids, gublerinids, racemiguembelinids, and pseudotextularids) during the climate warming of zones CF1-2 between 65.4 and 65.2 Ma (Li and Keller, 1998a,b). Abramovich and Keller (2003) observed that most ecological specialists are dwarfed during this warm event at Site 525 in the middle latitude South Atlantic. However, the low-diversity postvolcanism late Maastrichtian assemblages of Site 216 are unknown from similar middle latitude localities in either shallow restricted or deeper open ocean environments (see Section 7.2).

8. Discussion

8.1. Mass extinctions impacts and volcanism

Most major mass extinctions in Earth's history are associated with large igneous provinces (Courtillot, 1999; Courtillot et al., 1996; Kerr, 1998; Wignall, 2001; Courtillot and Renne, 2003). Only the K–T boundary mass extinction is generally recognized as a direct consequence of a large impact event and Chicxulub has been identified as the impact crater. Recent studies suggest that Chicxulub is not the K–T impact crater, but rather one of several impacts (Keller et al., 2003, 2004a,b), and that flood basalt volcanism can cause the same catastrophic biotic effects as large impacts (Keller et al., 2003, this study). This raises the possibility that Deccan volcanism may have contributed as much (or more) as one or more impacts to the demise of the dinosaurs and other organisms at the end of the Cretaceous. A number of studies have discussed the similar environmental effects caused by volcanism and impacts, including greenhouse warming, acid rain, and eutrophication (e.g., O'Keefe and Ahrens, 1989; Caldeira and Rampino, 1990; Sigurdsson et al., 1992; Sutherland, 1994). Here we focus on the long-term records of the mass extinction, impacts, and volcanism of the Cretaceous–Tertiary transition.

8.2. K–T mass extinction

The most prominent victims of the K–T mass extinction are the dinosaurs, which declined in diversity from the late Campanian through the Maastrichtian, and the last members of this group arguably disappeared at or near the K–T boundary (Archibald, 1996). Almost all other faunal groups reveal similar gradual or progressive diversity changes during the late Maastrichtian, which are attributed to long-term climatic and environmental changes (see reviews in MacLeod et al., 1997; Keller, 2001). In fact, only planktic foraminifera record a sudden mass extinction at the K–T boundary coincident with the onset of the boundary clay layer, an iridium anomaly, major negative $\delta^{13}C$ excursion, drop in $CaCO_3$, and increased total organic matter. What is generally missed, however, is that extinctions affected only ecologically sensitive tropical and subtropical species, and although this group comprised 66% of the total species population, their combined total abundance was less than 10% of the foraminiferal population during the last 500 kyr of the Maastrichtian. Focusing on the K–T boundary extinctions alone therefore misses the onset and probable cause(s) of the environmental perturbation that eventually led to the mass extinction. The end-Cretaceous mass extinction began during the last 500 kyr of the Maastrichtian and accelerated during the last 100 kyr, as evident in the remarkably similar species richness patterns of planktic foraminifera, ammonites, bivalves, and palynoflora, although only inoceramids and rudistids suffered major extinctions during this time (review in Keller, 2001).

Attributing this progressive or gradual extinction pattern to a single bolide impact at the K–T boundary is the source of continued controversy. There is

undeniable geochemical and geophysical evidence of a large impact on the Yucatan Peninsula 65 myr ago, but there is equally undeniable evidence of bones and shells of creatures that died out well prior to the K–T boundary and therefore cannot be attributed to it. Deccan traps and Ninetyeast Ridge volcanism are well documented for the late Maastrichtian and, as this study shows, at least, regionally caused the same catastrophic biotic effects as at the K–T boundary, which coincided with major Deccan volcanism and an impact. Therefore, the existence of an impact alone can no longer be considered sufficient evidence to explain the K–T mass extinction. The accumulating evidence of multiple impacts and their environmental effects have yet to be considered, although no dramatic environmental or biotic changes have been observed, except at the K–T boundary. The flood basalt extinction hypothesis gains much support from the paleontological record because the timing and duration are compatible with the progressive extinction record. However, the environmental ramifications of flood basalt eruptions and the associated biotic effects have been difficult to quantify (see reviews in Wignall (2001) and Keller (in press)).

8.3. Multiple impacts

The K–T boundary is defined by the mass extinction of all tropical and subtropical planktic foraminifera, a boundary clay and basal thin red layer that usually contains an iridium anomaly, the first appearance of Danian species near the base of the boundary clay, and a 2–3‰ negative carbon isotope excursion (Keller et al., 1995). Identification of the K–T boundary is thus independent of impact ejecta, which allows us to avoid the circular reasoning that because impact ejecta is present (iridium anomaly, microtektites, shocked quartz), it must be the K–T boundary. Not all impact ejecta layers are of K–T boundary age. Increasingly, the stratigraphic position of ejecta layers reveals the presence of multiple impacts during the late Maastrichtian to early Danian.

The K–T boundary impact is the most prominent and well-documented event associated with a major mass extinction. The Chicxulub crater on Yucatan, Mexico, is generally considered the impact that caused the end-Cretaceous mass extinction. Impact ejecta (microtektites) near the K–T boundary in sections from northeastern Mexico, with $^{40}Ar/^{39}Ar$ ages of 65.0 Ma and an error margin of plus or minus 200 kyr, are the primary evidence for a K–T age. However, microtektite layers have recently been found interbedded in late Maastrichtian sediments throughout northeastern Mexico, with the oldest layer in undisturbed pelagic marls near the base of zone CF1, which spans the last 300 kyr of the Maastrichtian. This indicates that the Chicxulub impact predates the K–T boundary by about 300 kyr (Keller et al., 2002b, 2003a).

The new core Yaxcopoil-1 drilled inside the Chicxulub crater also yields a pre-K–T age for the Chicxulub impact based on stratigraphic, paleomagnetic, and stable isotopic analyses (Keller et al., 2004a,b). In this core, the K–T boundary is uncontroversially identified by a thin green glauconitic clay layer at 50 cm above the impact breccia and coincident with the disappearance of Cretaceous planktic foraminiferal species. The first early Danian species appear immediately above this clay layer. The controversial part concerns the 50 cm between the K–T glauconitic clay layer and the top of the impact breccia. By interpreting this interval as backwash and crater infill, the impact breccia can be assumed to be coeval with the K–T boundary.

There are many reasons why the backwash interpretation is wrong. On a sedimentological basis, there is no evidence of high energy deposition, such as grain size grading, cross bedding, breccia clasts, clasts of underlying lithologies, and macrofossils and microfossils of the underlying platform paleoenvironments. Instead, the sediments consist of finely laminated dolomitic and micritic limestones, 1-cm thin layers of oblique bedding, and five thin green glauconitic and bioturbated layers below the K–T boundary (Keller et al., 2004a,b). Each of the glauconitic layers indicates that deposition occurred in gently agitated bottom waters and reduced sedimentation that permitted the formation of glauconite over an extended time interval. Each layer is also bioturbated, which indicates that the ocean floor was colonized by burrowing organisms during deposition. This sedimentation pattern cannot accommodate high-energy backwash and crater infill over a short time interval of days to weeks, but indicates deposition over an extended time interval.

The age of deposition can be determined from microfossils, paleomagnetic data, and carbon isotopes. Paleomagnetic data show deposition of the critical 50-

cm interval occurred in magnetochron C29r below the K–T boundary, and carbon isotope data indicate typical late Maastrichtian signals followed by the characteristic negative excursion across the K–T boundary. Planktic foraminiferal assemblages in the laminated micritic limestone below the K–T boundary are characteristic of zone CF1, which spans the last 300 kyr of the Maastrichtian (Keller et al., 2004a). There is no evidence that these assemblages are reworked because no species older than zone CF1 are present, and no planktic foraminifera lived in the shallow platform carbonate of the Cretaceous prior to the Chicxulub impact. Thus, the paleomagnetic, stable isotope and microfossil data all support deposition during the last 300 kyr of the Maastrichtian, whereas sedimentologic data indicate normal low energy pelagic deposition. These data show that Chixculub is not the K–T boundary impact crater, but an earlier pre-K–T impact event. No species extinctions are associated with this event. The late Maastrichtian greenhouse warming began prior to deposition of the Chicxulub impact ejecta and appears to be related to Deccan volcanism.

A multiple impact scenario across the K–T transition is also supported by recent discoveries of two small impact craters of late Maastrichtian age in the North Sea (Silverpit) and Ukraine (Kelley and Gurov, 2002; Stewart and Allen, 2002), and two Ir anomalies in Oman (Ellwood et al., 2003). Other impact craters that have been associated with the K–T boundary include Manson (Iowa) and Kara (Western Sibiria). There is also evidence of an impact in the early Danian based on Ir anomalies in the *P. eugubina* zone (Pla) in five Central American localities (Bochil Coxquihui and Trinitaria in Mexico, Actela, Guatemala, and Beloc, Haiti; Stueben et al., 2002; Keller et al., 2003). The temporal and global distribution of these impacts argues against the breakup of a parent asteroid with smaller chunks hitting the Earth simultaneously. Van Flandern (1999, written communication, CCNET 11/5/03) argues that the cluster of craters more likely implies the explosion of a planet-sized parent body in the main asteroid belt for which there is considerable astronomical evidence (Napier, 2001).

Although multiple impacts can now be identified in late Maastrichtian, K–T and early Danian deposits, only the K–T boundary is associated with a mass extinction. The biotic effects of the other impacts, including Chicxulub, caused no species extinctions and the biotic stress may have been short-term (Keller, in press).

8.4. Volcanism

Volcanism during the late Maastrichtian appears to have been the primary cause for the climate change, including the greenhouse warming and associated global stress-induced species dwarfing (Li and Keller, 1998a,b; Kucera and Malmgren, 1998; Olsson et al., 2001; Abramovich and Keller, 2002, 2003). However, only now can we directly link specific biotic effects to volcanism based on the volcanic sediments of Ninetyeast Ridge Site 216. At this locality, the high-stress dwarfed planktic foraminiferal assemblages within the volcanic sediments provide proxies for evaluating the biotic effects of volcanism. In particular, the disaster opportunist *Guembelitria* blooms are proxies for the most severe biotic stress conditions, whereas the low O_2 ecological generalists (heterohelicids) mark initial recovery phases.

From the Indian Ocean to the Tethys, a pattern of disaster and initial recovery repeats itself through the late Maastrichtian and early Danian, but only minor effects are recognized in Tunisia (shaded interval in Fig. 6; Keller et al., 2003). Only rare *Guembelitria* have been observed in Spain or Italy, although they are particularly abundant in Bulgaria (Adatte et al., 2002). This suggests a westward decrease in the intensity of environmental effects of volcanism in the Indian Ocean. Three such disaster/recovery horizons have been recognized in late Maastrichtian (zones CF1–CF3) sediments of Israel and Tunisia, two in Egypt where the middle recovery event (zone CF2) is missing, but only one is present (zone CF3) in Madagascar due to hiatuses (Fig. 6). The same alternating disaster/recovery pattern is repeated in the early Danian. Periods of intense Deccan volcanism (Courtillot, 1999; Hoffmann et al., 2000) correlate well with periods dominated by disaster opportunists, suggesting that *Guembelitria* blooms are directly related to the intensity of volcanism with recovery periods related to decreased volcanic input. This indicates statistical universality in the planktic foraminiferal response to high-stress environments independent of time or cause(s)—whether impacts or volcanism.

The evidence indicates that volcanism can induce catastrophic biotic effects similar to those commonly attributed to the K–T mass extinction. This leads to the inevitable question: Was the K–T mass extinction caused by an impact or volcanism? At this time, the evidence suggests that it was a combination of impacts and volcanism, rather than one or the other.

8.5. Further studies

Guembelitria blooms are reliable proxies for environmental catastrophes during the late Maastrichtian and post-K–T early Danian. Quantifying this easily identifiable small species thus provides a simple method for recognizing times of high environmental stress. Its geographic distribution can locate areas of maximum stress and hence can lead to the source of the environmental perturbation. The first-order investigation should concern the temporal and geographic distributions of *Guembelitria* blooms during the late Maastrichtian and K–T boundary and its association with flood basalts and/or impacts. While the geographic distribution of this disaster opportunist is well documented for the K–T boundary event (Fig. 7), little is known of its spatial and temporal distribution in other time intervals, particularly during the late Maastrichtian. This is largely because routine species analysis does not include the small size fraction (38–100 μm) that contains *Guembelitria* and several small low O_2-tolerant biserial species. A major effort is required to investigate the small size fraction (38–100 μm) for the late Maastrichtian across latitudes to reveal background levels, crisis response, and latitudinal distribution of these species.

Since *Guembelitria* species are very long-ranging and appear to have remained disaster opportunists, this proxy can identify environmental catastrophes from the middle Cretaceous to the Recent. A systematic analysis of species in the small size fraction (38–100 μm) in marine sequences associated with large igneous provinces would document the environmental stress associated with major volcanism. Documenting the presence of disaster taxa from the late Cretaceous should also reveal additional environmental catastrophes, as for example during the Albian, the Cenomanian–Turonian transition, and the Campanian (Kroon and Nederbragt, 1990; Kerr, 1998; Keller, 2001).

Little is known of the environmental conditions that lead to *Guembelitria* blooms. Preliminary $\delta^{13}C$ species ranking suggests that *Guembelitria* species are isotopically the lightest species living in surface waters and thriving in eutrophic environments (Barrera and Keller, 1994). Further geochemical studies are needed to determine the environmental conditions, including (1) stable isotope analysis of *Guembelitria* tests relative to other species in order to determine the isotopic ranking, productivity, and temperature conditions; (2) trace element analysis of benthic and planktic foraminiferal tests to determine toxicity levels that may have proved lethal for specialized species; and (3) evaluation of nutrient, salinity, temperature, and oxygen variations.

9. Conclusions

During the late Maastrichtian, DSDP Site 216 on Ninetyeast Ridge, Indian Ocean, passed over a mantle plume, leading to volcanic eruptions, islands built to sea level, and catastrophic regional environmental conditions for planktic and benthic foraminifera. The biotic effects of this mantle plume volcanism were severe, including dwarfing of all benthic and planktic species, extremely low species richness (6–10 species), 90% reduced species diversity, exclusion of all ecological specialists, near-absence of ecological generalists in surface waters, and dominance of *Guembelitria* blooms alternating with low O_2-tolerant species. These faunal characteristics are nearly identical to those of the K–T boundary mass extinction, except that the fauna recovered after Site 216 passed beyond the influence of mantle plume volcanism about 500 kyr before the K–T boundary.

Blooms of the disaster opportunist *Guembelitria* are a proxy for environmental catastrophes, leading to severe biotic stress conditions that may range from temporary exclusion of ecological specialists and generalists to mass extinctions. The ecological generalists consisting of small biserial species (*Heterohelix globulosa*, *H. navarroensis*, *H. dentata*, and *Z. waiparaensis*) are proxies for low O_2 conditions and mark initial recovery. Continued recovery of the ecosystem is indicated by increasing abundance of small trochospiral and planispiral ecological generalists in surface waters (hedbergellids, globigerinellids,

R. rugosa, and *R. macrocephala*). Return to more normal environmental conditions is indicated by the reappearance of larger (>150 μm) specialized tropical or subtropical species after volcanic influx ceased during the late Maastrichtian. These ecological specialists suffered total extinction during the K–T mass extinction. The direct correlation between mantle plume volcanism and biotic effects on Ninetyeast Ridge and the similarity to the K–T mass extinction, which is generally attributed to a large impact, reveals that impacts and volcanism can cause similar environmental catastrophes.

Acknowledgments

I gratefully acknowledge comments by Stephen Hesselbo and one anonymous reviewer, as well as discussion with Abdel Tantawy, Thierry Adatte, Silvia Gardin, and Sigal Abramovich. This study was supported by NSF grant EAR-0207407. DSDP samples were provided by the Ocean Drilling Program.

References

Abramovich, S., Keller, G., 2002. High stress late Maastrichtian paleoenvironment: inferences from planktic foraminifera in Tunisia. Palaeogeogr. Palaeoclimatol. Palaeoecol. 178, 145–164.

Abramovich, S., Keller, G., 2003. Planktic foraminiferal response to the latest Maastrichtian abrupt warm event: a case study from South Atlantic DSDP Site 525A. Mar. Micropaleontol. 48, 225–249.

Abramovich, S., Almogi, L.A., Benjamini, C., 1998. Decline of the Maastrichtian pelagic ecosystem based on planktic Foraminifera assemblage change; implication for the terminal Cretaceous faunal crisis. Geology 26 (1), 63–66.

Abramovich, S., Keller, G., Adatte, T., Stinnesbeck, W., Hottinger, L., Stueben, D., Berner, Z., Ramanivosoa, B., Randriamanantenasoa, A., 2002. Age and paleoenvironment of the Maastrichtian–Paleocene of the Mahajanga basin, Madagascar: a multidisciplinary approach. Mar. Micropaleontol. 47, 17–70.

Abramovich, S., Keller, G., Stueben, D., Berner, Z., 2003. Characterization of late Campanian and Maastrichtian planktic foraminiferal depth habitats and vital activities based on stable isotopes. Paleogeogr., Paleoclimatol., Paleoecol. 202, 2–29.

Adatte, T., Keller, G., Burns, S., Stoykova, K.H., Ivanov, M.I., Vangelov, D., Kramar, U., Stueben, D., 2002. Paleoenvironment across the Cretaceous–Tertiary transition in eastern Bulgaria. Spec. Pap.-Geol. Soc. Am. 356, 231–252.

Archibald, J.D., 1996. Testing extinction theories at the Cretaceous/Tertiary boundary using the vertebrate fossil record. In: MacLeod, N., Keller, G. (Eds.), Cretaceous–Tertiary Mass Extinction: Biotic and Environmental Changes. W.W. Norton and Co, New York, pp. 373–399.

Barrera, E., Keller, G., 1994. Productivity across the Cretaceous–Tertiary boundary in high latitudes. Geol. Soc. Amer. Bull. 106, 1254–1266.

Caldeira, G.K., Rampino, M.R., 1990. Deccan volcanism, greenhouse warming and the Cretaceous/Tertiary boundary. Spec. Pap.-Geol. Soc. Am. 247, 117–123.

Caron, M., 1985. Cretaceous planktic foraminifera. In: Bolli, H.M., Saunders, J.B., Perch Nielsen, K. (Eds.), Plankton Stratigraphy. Cambridge University Press, Cambridge, pp. 17–86.

Courtillot, V.E., 1999. Evolutionary Catastrophes: The Science of Mass Extinction. Cambridge University Press. 174 pp.

Courtillot, V.E., Renne, P.R., 2003. On the ages of flood basalt events. Geodyn. C. R. Geosci. 335, 113–140.

Courtillot, V.E., Jaeger, J.J., Yang, Z., Feraud, G., Hofmann, C., 1996. The influence of continental flood basalts on mass extinctions: where do we stand? Spec. Pap.-Geol. Soc. Am. 307, 513–526.

Culver, S.J., 2003. Benthic foraminifera across the Cretaceous–Tertiary boundary: a review. Mar. Micropaleontol. 47, 177–226.

Dercourt, J., Ricou, L.E., Vrielynck, B., 1993. Atlas Tethys Paleoenvironmental Maps. Gauthier-Villars, Paris. 307 pp.

Ellwood, B.B., MacDonald, W.D., Wheeler, C., Benoist, S.L., 2003. The K–T boundary in Oman: identified using magnetic susceptibility field measurements with geochemical confirmation. EPSL 206, 529–540.

Gardin, S., Monechi, S., 1998. Paleoecological change in middle to low-latitude calcareous nannoplankton at the Cretaceous/Tertiary boundary. Bull. Soc. Géol. Fr. 169 (5), 709–723.

Gartner Jr., S., 1974. Nannofossil biostratigraphy Leg 22, Deep Sea Drilling Project. In: von der Borch, C.C., Slater, J.G., et al. (Eds.), Initial Reports of the Deep Sea Drilling Project, vol. 22. U.S. Government Printing Office, Washington, pp. 577–600.

Gartner Jr., S., Johnson, D.A., McGowran, B., 1974. Paleontology synthesis of deep sea drilling results from Leg 22 in the northeastern Indian Ocean. In: von der Borch, C.C., Slater, J.G., et al. (Eds.), Initial Reports of the Deep Sea Drilling Project, vol. 22. U.S. Government Printing Office, Washington, pp. 805–813.

Hekinian, R., 1974. Petrology of igneous rocks from Leg 22 in the northeastern Indian Ocean. In: von der Borch, C.C., Slater, J.G., et al. (Eds.), Initial Reports of the Deep Sea Drilling Project, vol. 22. U.S. Government Printing Office, Washington, pp. 412–448.

Hoffmann, C., Feraud, G., Courtillot, V.E., 2000. $^{40}Ar/^{39}Ar$ dating of mineral separates and whole rocks from the Western Ghats lava pile: further constraints on duration and age of Deccan Traps. EPSL 180, 13–27.

Keller, G., 1989. Extended Cretaceous/Tertiary boundary extinctions and delayed population change in planktonic foraminifera from Brazos River, Texas. Paleoceanography 4, 287–332.

Keller, G., 1992. Paleoecologic response of Tethyan benthic foraminifera to the Cretaceous–Tertiary boundary transition. Studies in Benthic Foraminifera, BENTHOS '90, Sendai, Japan, 1990. Tokai University Press, Sendai, Japan, pp. 77–91.

Keller, G., 1993. The Cretaceous/Tertiary boundary transition in the Antarctic Ocean and its global implications. Mar. Micropaleontol. 21, 1–45.

Keller, G., 2001. The end-Cretaceous mass extinction in the marine realm: year 2000 assessment. Planet. Space Sci. 49, 817–830.

Keller, G., 2002. *Guembelitria* dominated late Maastrichtian planktic foraminiferal assemblages mimic early Danian in Central Egypt. Mar. Micropaleontol. 47, 71–99.

Keller, G., 2003. Biotic effects of volcanism and impacts. Earth Planet. Sci. Lett. 215, 249–264.

Keller, G., 2004. Low diversity late Maastrichtian and early Danian planktic foraminiferal assemblages of the eastern Tethys. J. Foraminiferal Res. 34, 49–73.

Keller, G., in press. Mass Extinctions, Impacts and Volcanism - Coincidence or cause-effect? Australian Journal of Earth Sciences (AJES).

Keller, G., Barrera, E., Schmitz, B., Matsson, E., 1993. Gradual mass extinction, species survivorship, and long term environmental changes across the Cretaceous–Teriary boundary in high latitudes. Geol. Soc. Amer. Bull. 105, 979–997.

Keller, G., Li, L., MacLeod, N., 1995. The Cretaceous–Tertiary boundary stratotype section at El Kef, Tunisia: how catastrophic was the mass extinction? Palaeogeogr. Palaeoclimatol. Palaeoecol. 119, 221–254.

Keller, G., Adatte, T., Stinnesbeck, W., Stueben, D., Kramar, U., Berner, Z., Li, L., von Salis Perch Nielsen, K., 1998. The Cretaceous–Tertiary transition on the shallow Saharan platform of southern Tunisia. GEOBIOS 30 (7), 951–975.

Keller, G., Adatte, T., Stinnesbeck, W., Luciani, V., Karoui-Yaakoub, N., Zaghbib-Turki, D., 2002a. Paleoecology of the Cretaceous–Tertiary mass extinction in planktonic foraminifera. Palaeogeogr. Palaeoclimatol. Palaeoecol. 178, 257–297.

Keller, G., Adatte, T., Stinnesbeck, W., Affolter, M., Schilli, L., Lopez-Oliva, J.G., 2002b. Multiple spherule layers in the late Maastrichtian of northeastern Mexico. Spec. Pap.-Geol. Soc. Am. 356, 145–161.

Keller, G., Stinnesbeck, W., Adatte, T., Stueben, D., 2003. Multiple impacts across the Cretaceous–Tertiary boundary. Earth Sci. Rev. 62, 327–363.

Keller, G., Adatte, T., Stinnesbeck, W., Rebolledo-Vieyra, M., Urrutia-Fucugauchi, J., Kramar, U., Stueben, D., 2004a. Chicxulub impact predates the K–T boundary mass extinction. Proceedings of the National Academy of Sciences of the United States of America (PNAS) 101 (11), 3721–3992.

Keller, G., Adatte, T., Stinnesbeck, W., Stueben, D., Berner, Z., Kramar, U., Harting, M., 2004b. More evidence that the Chicxulub impact predates the K–T boundary mass extinction. Meteoritics & Planetary Sciences 39 (7), 1127–1144.

Kelley, P.S., Gurov, E., 2002. Boltysh, another end-Cretaceous impact. Meteorit. Planet. Sci. 37, 1031–1043.

Kerr, A.C., 1998. Oceanic plateau formation: a cause of mass extinction and black shale deposition around the Cenomanian–Turonian boundary? J. Geol. Soc. Lond. 155, 619–626.

Kroon, D., Nederbragt, A.J., 1990. Ecology and paleoecology of triserial planktic foraminifera. Mar. Micropaleontol. 16, 25–38.

Kucera, M., Malmgren, B.A., 1998. Terminal Cretaceous warming event in the mid-latitude South Atlantic Ocean: evidence from poleward migration of *Contusotruncana contusa* (planktonic foraminifera) morphotypes. Palaeogeogr. Palaeoclimatol. Palaeoecol. 138, 1–15.

Li, L., Keller, G., 1998a. Maastrichtian climate, productivity and faunal turnovers in planktic foraminifera in South Atlantic DSDP Sites 525 and 21. Mar. Micropaleontol. 33, 55–86.

Li, L., Keller, G., 1998b. Abrupt deep-sea warming at the end of the Cretaceous. Geology 26, 995–999.

Li, L., Keller, G., Adatte, T., Stinnesbeck, W., 2000. Late Cretaceous sea level changes in Tunisia: a multi-disciplinary approach. J. Geol. Soc. Lond. 157, 447–458.

MacLeod, N., Rawson, P.F., Forey, P.L., Banner, F.T., Boudagher-Fadel, M.K., Bown, R.R., Burnett, J.A., Chambers, P., Culver, S., Evans, S.E., Jeffrey, C., Kaminski, MA., Lord, A.R., Milner, A.C., Milner, A.R., Morris, N., Own, E., Rosen, B.R., Smith, A.B., Taylor, P.D., Urquhart, E., Young, J.R., 1997. The Cretaceous–Tertiary biotic transition. J. Geol. Soc. Lond. 154, 265–292.

MacLeod, N., Ortiz, N., Fefferman, N., Clyde, W., Schulter, C., MacLean, J., 2000. Phenotypic response of foraminifera to episodes of global environmental change.. In: Culver, S.J., Rawson, P. (Eds.), Biotic Response to Global Environmental Change: The Last 145 Million Years. Cambridge University Press, Cambridge, pp. 51–78.

McDougall, I., 1974. Potassium–argon ages on basaltic rocks recovered from DSDP Leg 22, Indian Ocean. In: von der Borch, C.C., Slater, J.G., et al. (Eds.), Initial Reports of the Deep Sea Drilling Project, vol. 22. U.S. Government Printing Office, Washington, pp. 377–380.

McGowran, B., 1974. Foraminifera. In: von der Borch, C.C., Slater, J.G., et al.,Initial Reports of the Deep Sea Drilling Project, vol. 22. U.S. Government Printing Office, Washington, pp. 609–628.

Meudt, M., Berner, Z., Kramar, U., Stüben, D., Keller, G., 2003. Hydrothermal influence on benthic foraminiferal geochemistry: evidence from DSDP—Site 216, Ninetyeast Ridge, Indian Ocean. Mantle Plumes: Physical Processes, Chemical Signatures, Biological Effects, Meeting, September 10–11, Cardiff University/National Museum and Gallery, Cardiff, Abstract.

Moore, D.G., Curray, J.R., Raitt, R.W., Emmel, F.J., 1974. Stratigraphic–seismic sections correlations and implications to Bengal fan history. In: von der Borch, C.C., Slater, J.G., et al. (Eds.), Initial Reports of the Deep Sea Drilling Project, vol. 22. U.S. Government Printing Office, Washington, pp. 403–412.

Murray, J.W., 2003. Patterns in cumulative increase in species from foraminiferal time series. Mar. Micropaleontol. 48, 1–21.

Napier, W.M., 2001. The influx of comets and their debris. In: Peucker-Ehrenbrink, B., Schmitz, B. (Eds.), Accretion of Extraterrestrial Matters Throughout Earth's History. Kluwer, Dordrecht, pp. 51–74.

Nederbragt, A.J., 1991. Late Cretaceous biostratigraphy and development of Heterohelicidae (planktic foraminifera). Micropaleontology 37, 329–372.

Nederbragt, A.J., 1992. Paleoecology of late Maastrichtian Heterohelicidae (planktic foraminifera) from the Atlantic region. Palaeogeogr. Palaeoclimatol. Palaeoecol. 92, 361–377.

Nederbragt, A.J., 1998. Quantitative biogeography of late Maastrichtian planktic foraminifera. Micropaleontology 44 (4), 385–412.

O'Keefe, J.D., Ahrens, J.T., 1989. Impact production of CO_2 by the Cretaceous/Tertiary extinction bolide and the resultant heating of the Earth. Nature 338, 247–348.

Olsson, R.K., Hemleben, C., Berggren, W.A., Huber, B.T., 1999. Atlas of Paleocene planktonic foraminifera. Smithsonian Contribution to Paleobiology, vol. 85. Smithonian Institution Press, Washington, DC. 252 pp.

Olsson, R.K., Wright, J.D., Miller, K.D., 2001. Paleobiogeography of *Pseudotextularia elegans* during the latest Maastrichtian global warming event. J. Foraminiferal Res. 31, 275–282.

Pimm, A.C., 1974. Sedimentology and history of the northeastern Indian Ocean from late Cretaceous to Recent. In: von der Borch, C.C., Slater, J.G., et al. (Eds.), Initial Reports of the Deep Sea Drilling Project, vol. 22. U.S. Government Printing Office, Washington, pp. 717–804.

Robaszynski, F., Caron, M., Gonzalez Donoso, J.M., Wonders, A.A.H., 1983-1984. Atlas of Late Cretaceous globotruncanids. Micropaleontology 26 (3-4), 145–305.

Schmitz, B., Keller, G., Stenvall, O., 1992. Stable isotope and foraminiferal changes across the Cretaceous–Tertiary boundary at Stevns Klint, Denmark: arguments for long-term oceanic instability before and after bolide impact. Palaeogeogr. Palaeoclimatol. Palaeoecol. 96, 233–260.

Sigurdsson, H., D'Hondt, S., Carey, S., 1992. The impact of the Cretaceous/Tertiary bolide on evaporite terrane and generation of major sulfuric acid aerosol. Earth Planet. Sci. Lett. 109, 543–559.

Stewart, S.A., Allen, J.P., 2002. A 20-km-diameter multi-ringed impact structure in the North Sea. Nature 418, 520–523.

Stueben, D., Kramar, U., Berner, Z., Eckhardt, J.D., Stinnesbeck, W., Keller, G., Adatte, T., Heide, K., 2002. Two anomalies of platinum group elements above the Cretaceous–Tertiary boundary at Beloc, Haiti: geochemical context and consequences for the impact scenario. Spec. Pap.-Geol. Soc. Am. 356, 163–188.

Sutherland, F.L., 1994. Volcanism around K/T boundary time—its role in an impact scenario for the K/T extinction events. Earth Sci. Rev. 36, 1–26.

Tantawy, A.A.A., 2002. Calcareous nannofossil biostratigraphy and paleoecology of the Cretaceous–Tertiary transition in the western desert of Egypt. Mar. Micropaloentol. 47, 323–356.

Tantawy, A.A.A., 2003. Maastrichtian calcareous nannofossil biostratigraphy and paleoenvironment of the Mahajanga Basin, Madagascar. Geology of Africa, 3rd Proceedings, Assiut University, Assiut, December 7.

Tantawy, A.A.A., Keller, G., 2003. Biotic effects of volcanism on calcareous nannofossils and planktic foraminifera: Ninetyeast Ridge, Indian Ocean. Egyptian Journal of Paleontology 3, 1–23.

Thompson, G., Bryan, W.B., Frey, F.A., Sung, A.C., 1974. Petrology and geochemistry of basalts and related rocks from sites 214, 215, 217 DSDP Leg 22, Indian Ocean. In: von der Borch, C.C., Slater, J.G., et al. (Eds.), Initial Reports of the Deep Sea Drilling Project, vol. 22. U.S. Government Printing Office, Washington, pp. 459–468.

Van Flandern, T., 1999. Dark Matter, Missing Planets and New Comets. Synthesis of Exploded Planet Hypothesis (EPH) Evidence, (2nd ed.)North Atlantic Books, Berkeley. Chapter 11.

Von der Borch, C.C., Sclater, J.G., et al., 1974. Site 216. Initial Reports of the Deep Sea Drilling Project, vol. 22. U.S. Government Printing Office, Washington, pp. 213–266.

Von Morkhoven, F.P.C.M., Berggren, W.A., Edwards, A.S., 1986. Cenozoic cosmopolitan deep-water benthic foraminifera. Bull. Cent. Rech. Explor. Prod. Elf-Aquitaine, Mem. 11 (421 pp.).

Wignall, P.B., 2001. Large igneous provinces and mass extinctions. Earth Science Reviews 53, 1–33.